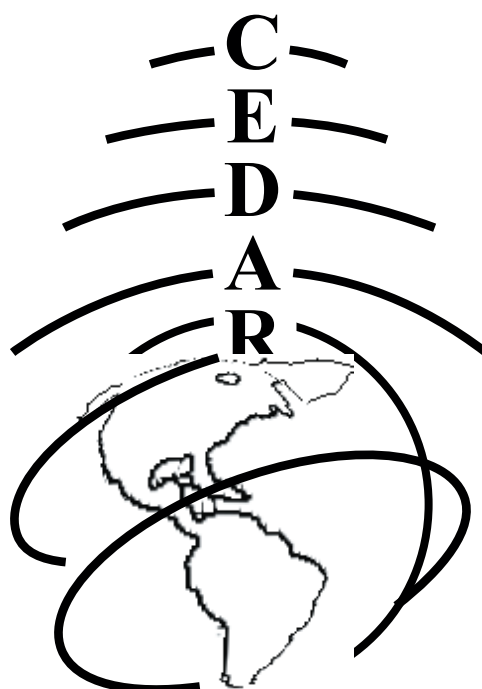


2008 CEDAR Workshop
Zermatt Resort and Spa
Midway, Utah, USA
June 16 - 21, 2008



Thursday CEDAR Poster Session Booklet
June 19



Zermatt Resort, Utah

Table of Contents

I. Instruments or Techniques for Ionosphere or Thermosphere Observation

ITIT-01, James Clemmons, Paired Ionosphere-Thermosphere Orbiters (PITO): A general-purpose science mission with high capability	1
ITIT-02, Cheng-Yung Huang Latitudinal Variation of High latitude Localized Neutral Density for Quiet Geomagnetic Conditions	1
ITIT-03, John Meriwether, Plans for ion-neutral coupling studies utilizing the Alaskan Fabry-Perot Interferometer network and the AMISR radar	1
ITIT-04, Edwin J Mierkiewicz A multi-line investigation aimed at deriving hydrogen densities in the upper atmosphere	2
ITIT-05, Serge Minin, Alignment of a remote all-sky triple-etalon Doppler imaging system: techniques and challenges	2
ITIT-06, Dominik Pilinski, Analysis of a Novel Approach for Determining Atmospheric Density from Satellite Drag	2
ITIT-07, Rob Redmon NGDC Ionosonde Program	3
ITIT-08, Steve Mende, presented by Tom Immel, Neutral Ion Coupling Explorer (NICE) – a NASA SMall Explorer Mission	3
ITIT-09, Christopher Watts, Modeling Ionospheric Effects for the LWA	4
ITIT-10, by K. F. Dymond, presented by L. J Rickard, The Combined Radio Interferometry and COSMIC Experiment in Tomography (CRICKET) Campaign	4
ITIT-11, Nick Zabotin, Principles of Dynasonde Data Acquisition and Processing	4
ITIT-12, Nick Zabotin, Spatial Effects of Multiple Scattering of HF Signals in the Ionosphere: Theory and Experiment	5
ITIT-13, Shaun Armstrong, Observing the coupling of ionospheric irregularities and thermospheric neutral dynamics using Fabry-Perot observatories: a new approach	5
ITIT-14, Richard Todd Parris, Recent Upgrades to the Kodiak Island SuperDARN Radar	5
ITIT-15, Jeffrey Spaleta, Enhanced Line of Sight Velocity Analysis Using an Aperiodic Pulse Sequence on the Kodiak and King Salmon Radars	5

II. Long Term Variations of the Upper Atmosphere

LTRV-01, Christiano Garnett Marques Brum, Solar cycles and geomagnetic variability of nighttime topside hydrogen, oxygen and helium ion fractions over Arecibo	6
LTRV-02, Eva Robles, presented by Ethan Engle Solar, geomagnetic and seasonal variability of the NmF2 and foF2 over Arecibo Observatory	6
LTRV-03, Goderdzi Didebulidze, presented by Nikoloz Gudadze, The long-term changes in the red 630.0 nm line nightglow intensity as an indicator of the dynamical changes in the upper atmosphere and decrease in the neutral gas density	6
LTRV-04, Susan M Nossal, Investigation of Solar Cyclic and Climatic Influences on Geocoronal Hydrogen	7
LTRV-05, John Noto, H-alpha Observations using Arecibo's new low resolution FPI	7
LTRV-06, Barbara Emery, Solar Wind Structure Sources and Periodicities of Global Electron Hemispheric Power over Three Solar Cycles	8

III. Solar Terrestrial Interactions in the Upper Atmosphere

SOLA-01, Ariel Acebal, Extending F10.7's Time Resolution to Capture Solar Flare Phenomena	8
SOLA-02, Seebany Datta-Barua, Deriving Neutral Winds from Global 4-D Electron Density Fields	8
SOLA-03, Kelly Ann Drake, Properties of the Ionospheric Signature of the Low-latitude Boundary Layer During Periods of Southward IMF	9
SOLA-04, Jiuhou Lei, Periodic Modulation of the Thermosphere by Solar Wind	9
SOLA-05, Anthony Mannucci, Local time dependence of the prompt ionospheric response for the November 2004 superstorms	10
SOLA-06, Brady O'Hanlon, GPS and Solar Radio Burst Forensics	10
SOLA-07, David Pawlowski, Modeling the thermospheric response to solar flares	10
SOLA-08, Liying Qian, Thermospheric and Ionospheric Response to Solar Flare Events	11
SOLA-09, Kate Roach, Altitude Dependence of Thermospheric Winds in HWM07	11
SOLA-10, Eric K Sutton, Latitudinal Response of Thermosphere Density to High-Latitude Heating	11
SOLA-11, Wenbin Wang, Storm-Time Comparisons of CMIT Results with GPS Data	11
SOLA-12, Justin Yonker, Fluorescence and Photodissociation of Nitric Oxide near 191 nm	12
SOLA-13, Marcos Diaz, Particle-In-Cell Simulation of Naturally Enhanced Ion Acoustic Lines Produced by an Electron Beam	12

IV. Polar Aeronomy

POLA-01, Robert Michell, High-resolution PFISR observations of NEIALs and associated auroral fine structures	12
POLA-02, Mark Conde, New results from the Poker Flat all-sky imaging Fabry-Perot spectrometer	13
POLA-03, Callum Anderson, presented by Mark Conde, Thermospheric Studies in Antarctica Using Fabry-Perot Spectrometers at Mawson and Davis Stations	13
POLA-04, Shaun Cooper, presentd by Mark Conde, Preliminary results of wave generation from a local scale thermospheric model	13
POLA-05, Thomas Butler, Volumetric imaging of the auroral ionosphere	13
POLA-06, Jose Fernandez, Storm/Quiet Ratio Comparisons Between TIMED/SABER NO+(v) Volume Emission Rates and Incoherent Scatter Radar Electron Densities at E-Region Altitudes	14
POLA-07, Jeffrey Holmes, The Velocity Filter Effect Observed in Cusp Proton Aurora	14
POLA-08, Irfan Azeem, Multi-instrument observations of dayside auroral emission dynamics at South Pole	15
POLA-09, Hamed Bekerat, Electron Precipitation Parameters and Ionospheric Conductances Inferred From Auroral Images Acquired by the Visible Imaging System (VIS) on the Polar Spacecraft	15
POLA-10, Christopher Fallen, Temporal evolution of the reflection height in response to HF heating in the polar ionosphere	15
POLA-11, Travis Gaulden, Observations of auroral-region energy dissipation by Joule heating as a function of spatial scale size	16
POLA-12, Peichen Lai, New Hardy Auroral Flux Model for Driving TIEGCM	16
POLA-13, Erik Lundberg, Plasma Wave and Particle Observations in a post Substorm Quiet Auroral Ionosphere	16
POLA-14, Astrid Maute, Influence of Spatial Structure of High-Latitude Joule Heating on Thermospheric Composition	17
POLA-15, Qian Wu, Resolute Optical Observation Current status and Future Plan	17
POLA-16, Matt Zettergren, Optical estimation of auroral ion upflow: A case study	17
POLA-17, Shasha Zou, Imaging ionospheric azimuthal flow bursts and the relationship to aurora using PFISR	18

V. Midlatitude Ionosphere or Thermosphere

MDIT-01, Stanley Briczinski, SHS Observations of O ⁺ : Initial Results	18
MDIT-02, Alan Burns, The behavior of the F2 peak ionosphere over the South Pacific at dusk during quiet summer conditions from COSMIC data	19
MDIT-03, Joseph Grebowsky, Radiation Belt Storm Probes Mission – An IT Community Asset?	19
MDIT-04, Xiaoli Luan, Mid-latitude nighttime enhancement in F-region electron density from global COSMIC measurements under solar minimum winter condition	19
MDIT-05, Clara Narvaez, Ionospheric Storms at a Sub-Auroral Location in the Southern Hemisphere	20
MDIT-06, Michi Nishioka, Super Medium-Scale Traveling Ionospheric Disturbance observed at mid-latitude during the geomagnetic storm on November 10, 2004	20
MDIT-07, Phil Richards, Backscattered fraction of precipitating ionospheric photoelectrons	21
MDIT-08, Ilgin Seker, Clues to the properties of medium scale traveling ionospheric discurbances	21
MDIT-09, David Voglozin, The Aeronomy of N ₂ ⁺ in the Earth's Ionosphere	21
MDIT-10, Steven Watchorn, Initial Spatial Heterodyne Spectrometer observations of neutral oxygen emission at 844.6 nm over Millstone Hill	21
MDIT-11, Preeti Bhaneja, Midlatitude spread F	22

VI. Equatorial Ionosphere or Thermosphere

EQUI-01, Shawn Adderly, Comparison of Coherent Backscatter and Airglow Images from Equatorial Plasma Depletion	22
EQIT-02, Narayan Chapagain, Simultaneous Observations of Equatorial Ionospheric Plasma Bubbles from Two Sites during the SpreadFex Campaign	22
EQIT-03, Jonathan Krall, Three-Dimensional Simulation of Equatorial Spread-F with Meridional Winds	23
EQIT-04, Akshay Malhotra, Effect of meteor ionization on Sporadic-E observed at Jicamarca	23
EQIT-05, Fabiano Rodrigues, Coherent scatter radar imaging observations of equatorial spread F in Brazil	23
EQIT-06, Yann Tambouret, Massively Parallel Simulations of Gradient Drift Waves in the E-region Ionosphere	23
EQIT-07, Patrick Alken, Estimating electric fields in the equatorial ionosphere from CHAMP observations	24
EQIT-08, Tzu-Wei Fang, Wind dynamo effects on ground magnetic perturbation and vertical drifts	24

EQIT-09, Freddy Galindo, presented by Karim Kuyeng, Improved E-region electron density and meridional wind measurements over Jicamarca using multi-static configurations.....	24
EQIT-10, Carlos Martinez, 630.0 nm airglow observations at mid-latitudes	
EQIT-11, Naomi Maruyama, Low Latitude Storm Time Electric Fields and their Role in the Coupled Thermosphere-Ionosphere Plasmasphere System.....	25
EQIT-12, Edgardo Pacheco, Variability of Zonal Ion Drifts During Storm-Times at Equatorial Latitudes	26
EQIT-13, Nicholas Pedatella, Longitudinal Structure of the Low-Latitude F-Region Ionosphere	26
EQIT-14, Pedrina Terra, Altitude Variation of the OII 7320Å spectral line width at Arecibo	26

Instruments or Techniques for Ionospheric or Thermospheric Observation

ITIT-01 Paired Ionosphere-Thermosphere Orbiters (PITO): A general-purpose science mission with high capability - by James Clemmons

Status of First Author: Non-student PhD

Authors: J. Clemmons, The Aerospace Corporation, james.clemmons@aero.org

Abstract: A mission that is capable of addressing many science topics in the realm of ionosphere-thermosphere physics is described and discussed. The mission utilizes a pair of orbiting vehicles in eccentric, high-inclination, coplanar orbits. The orbits have arguments of perigee that differ by 180 degrees and are phased such that one vehicle is at perigee (200 km) while the second is at apogee (2000 km). Half an orbit later, the vehicles switch positions. Three types of science instruments are envisioned to take advantage of this scenario: those that measure local, in-situ parameters, downlooking imagers that view areas, and vertical profiling instruments. The main idea is that in addition to the two-point measurements provided by the in-situ instrumentation, context information for the low-altitude measurements is obtained by the high-altitude imagers. In addition, profiling instruments such as sounders and spaceborne lidar can be added to create vertical profiles. Such an observation system is capable of providing elements of global coverage, regional coverage, and resolution in three dimensions. Presented are candidate orbits, strawman instrument suites, approximate mission resource needs, and expected science targets.

ITIT-02 Latitudinal Variation of High latitude Localized Neutral Density for Quiet Geomagnetic Conditions by Cheng-Yung Huang

Status of First Author: Non-student PhD

Authors: Cheng-Yung Huang, huangcn@bc.edu, Chin S. Lin, Chin.Lin@hanscom.af.mil, Frank A. Marcos, Frank.Marcos@hanscom.af.mil

Abstract: Thermospheric variations observed with satellite accelerometers near 400 km have shown localized structural features that have been associated with the polar cusp. To date only limited data sets have been presented and the cause of these variations has not been unambiguously determined. In this paper we used an extensive database of CHAMP neutral density measurements during 2001-2005 to examine the latitudinal variation of localized neutral density in the polar cusp region during very low magnetic conditions in terms of magnetic latitude-magnetic local time coordinates. Latitudinal dependence of solar flux effects during magnetic quiet times is also examined to establish a baseline for better understanding the geomagnetic effects on neutral density at dayside high latitude regions. The results provide new insights into the heating processes responsible for the localized density structures in the dayside cusp region.

ITIT-03 Plans for ion-neutral coupling studies utilizing the Alaskan Fabry-Perot Interferometer network and the AMISR radar - by John Meriwether

Status of First Author: Non-student

Authors: J. W. Meriwether, R. Hedden, M. Larsen (Clemson University), J. Herron, V. Wickwar (Utah State Univ.), L.L. Cogger (Univ. of Calgary) (john.meriwether@ces.clemson.edu)

Abstract: Ion-neutral coupling studies require accurate determination of the neutral wind vector as well as ion drift measurements. Common volume (CV) measurements by three FPI observatories represent an important tool by which the transfer of momentum by convecting plasma to the neutral atmosphere can be studied. There is no need to assume a symmetric wind field or that the vertical wind speed is small as all three components of the neutral wind vector within the common volume can be precisely determined. The three FPI locations that have been chosen are Poker, Ft. Yukon, and Eagle. A sequence of CV measurements over central Alaska with these observatories would provide measurements of the neutral wind vectors from which the scalar quantities of divergence and vorticity can be calculated. The variation of both of these quantities during a substorm would provide information regarding the relative importance of Joule heating and Lorentz forcing (ion-drag). The evolution of the polar thermosphere during the substorm can be regarded as the equivalence of a geostrophic adjustment in which the response of the thermosphere varies as the Rossby radius is modified by the large-scale structure of Joule heating and particle precipitation. The

three FPI observatories are undergoing construction and testing and are expected to be installed and operational by mid-August, 2006.

ITIT-04 A multi-line investigation aimed at deriving hydrogen densities in the upper atmosphere - by Edwin J Mierkiewicz

Status of First Author: Non-student

Authors: Edwin J. Mierkiewicz; UW-Madison; emierk@astro.wisc.edu, Fred L. Roesler; UW-Madison; roesler@wisp.physics.wisc.edu, Susan M. Nossal; UW-Madison; nossal@wisp.physics.wisc.edu

Abstract: We have obtained unprecedented sets of near-coincident measurements of extremely faint Balmer-alpha (656.3 nm) and Balmer-beta (486.1 nm) line intensities from Earth's geocorona with the Wisconsin H-alpha Mapper (WHAM), a highly sensitive Fabry-Perot spectrometer developed at the University of Wisconsin. In addition to WHAM, we are also operating a similarly designed, but higher resolution, Fabry-Perot at Pine Bluff Observatory (PBO) near Madison, WI. The PBO Fabry-Perot resolves the ~ 7 km/s full width at half maximum geocoronal Balmer-alpha and Balmer-beta line profiles, as well as providing intensity data. We have also developed modeling procedures following our work with James Bishop that when applied to these data sets provide a unique opportunity to determine the vertical distribution of hydrogen in the upper atmosphere, the vertical hydrogen transport flux, and the velocity partitioning of hydrogen atoms in the highest regions of the atmosphere.

In this poster we discuss these WHAM and PBO data sets and our strategies for coupled analysis of Balmer-alpha and Balmer-beta intensities and line profiles by forward radiative transport (RT) modeling. This multi-line analysis technique utilizes the differing transport properties of hydrogen Lyman-beta (primarily responsible for Balmer-alpha), and Lyman-gamma (primarily responsible for Balmer-beta) in the terrestrial atmosphere, and the forward-model/data comparisons of the variation of these emissions with viewing geometry, to constrain forward-model retrieved hydrogen density profiles and signatures of exospheric physics.

ITIT-05 Alignment of a remote all-sky triple-etalon Doppler imaging system: techniques and challenges by Serge Minin

Status of First Author: Student NOT in poster competition Masters

Authors: Serge Minin, Steve Watchorn, John Noto, Michael Migliozi

Abstract: A remotely operated all-sky triple-etalon Doppler imaging system for measuring wind velocities in the Earth's thermosphere is deployed at the Cerro Tololo Observatory. The instrument is designed to measure the 630.0 oxygen emission line. In order to obtain optimal transmission and resolution, a precision alignment of the component etalons has to be performed. Since the system is remotely operated, one-by-one alignment of the etalons (with the removal of the others) is not possible. Current technique involves a manual search through the domain of etalon pressures and subsequent optimization to obtain the maximum transmission at the center of the ring pattern. It is desirable, however, to develop an algorithm for quick and automatic alignment of the etalon to any transmission angle and wavelength in the vicinity. In this work we propose and discuss a model-based approach for detecting the phases of the three etalons from a set of measurements, and adjusting them for optimal transmission. This approach also contributes to an improved characterization and forward modeling of the instrument, which should be valuable for data analysis. The challenges, such as alignment for a wavelength different from the observation wavelength, as well as non-uniform calibration source are discussed.

ITIT-06 Analysis of a Novel Approach for Determining Atmospheric Density from Satellite Drag - by Marcin Dominik Pilinski

Status of First Author: Student IN poster competition PhD

Authors: Marcin Pilinski, Scott Palo

Abstract: Neutral density, composition, and wind measurements are increasingly needed to further scientific understanding of the upper atmosphere. To address this need, the model and error prediction of a low-cost system which makes in-situ measurements of the neutral atmosphere at altitudes of 350 - 200 km was developed. We present the errors involved in determining density from drag and look at improvements which can result from implementing a multi-instrument approach. The poster describes the models

developed in order to evaluate drag measurements in the thermosphere. As a case study we present simulation results for the Drag and Atmospheric Neutral Density Explorer (DANDE) spacecraft being developed at CU as a part of the Air Force sponsored University Nanosat Program. This spacecraft carries a novel drag measuring system which is evaluated in this study as well as a Wind and Temperature Spectrometer which measures the horizontal wind vector.

ITIT-07 NGDC Ionosonde Program - by Rob Redmon

Status of First Author: Student NOT in poster competition PhD

Authors: Rob Redmon - NOAA/NGDC (Rob.Redmon@noaa.gov), Jim Manley - CIRES/NGDC (James.Manley@noaa.gov), Eric Kihn - NOAA/NGDC (Eric.A.Kihn@noaa.gov), Terry Bullett - CIRES/NGDC (Terry.Bullett@noaa.gov), Justin Mabie - CIRES/NGDC (Justin.Mabie@noaa.gov)
Ray Conkright - CIRES/NGDC (Ray.O.Conkright@noaa.gov), William Denig - NOAA/NGDC (William.Denig@noaa.gov)

Abstract: The international Space Weather community has taken major financial hits in recent times. With the imminent canceling of important UK ground based instrument programs and the currently unfunded Air Force DISS network, the burden on the ionosonde community to bring our techniques and science further into public relevance is ever more imperative. The mission of the Solar and Terrestrial Physics division of the National Geophysical Data Center's (NGDC) ionosonde program is to improve the collection, analysis and dissemination of vertical incidence ionosonde measurements and derived data products independent of the data source. New instruments are being fielded, new data processing technologies are becoming practical, and historical records are being rescued. Through an effort to revitalize and prepare historical records for long term climate trending, over 2 million ionospheric measurements across 65 unique geographic locations have been formatted and prepared for public dissemination. But to continue to provide benefit to the space weather mission and space climate studies of National interest, and to have data to contribute to International efforts, the US must maintain a core ionosonde measurement capability with both operational relevance and scientific credibility. NOAA/NGDC stands ready to contribute to a US Ionosonde program, but needs assistance and contribution from other National Space Weather Program members.
We will present on accomplishments and new initiatives during this challenging period.

ITIT-08 Neutral Ion Coupling Explorer (NICE) – a NASA SMall Explorer Mission - by Steve Mende, presented by Tom Immel

Status of First Author: Non-student

Authors: Stephen B. Mende (UCB), Thomas Immel (UCB), Gary Swenson (UI) , Rod Heelis (UTF), Harald Frey (UCB), Jerry Edelstein (UCB), Geoffrey Crowley (ASTRA), Scott England (UCB), Jeffrey Forbes (U of Colorado), Joseph Huba (NRL), Farzad Kamalabadi (UI), Paul Kintner (Cornell), Jonathan Makela (UI), Mike Picone (NRL), Andrew Stephan (NRL), Jean-Claude Gerard (U of Liege), Benoit Hubert, (U of Liege), Pierre Rochus (U of Liege)

Abstract: NICE will discover how winds and composition of the upper atmosphere drive the electric fields and chemical reactions that control Earth's ionosphere. The goal of the NICE mission is to answer the central question: How do neutral dynamics drive ionospheric variability? The mission will resolve competing theories about the low-latitude ionospheric dynamo, and will explain how large-scale waves from the lower atmosphere can couple to the ionosphere and upper atmosphere. Understanding neutral-ion coupling in Earth's atmosphere has applications for solar and planetary atmospheres including Mars and Jupiter. NICE will be the first mission to simultaneously measure all the key parameters that both characterize and drive the ionosphere. It will remotely measure the neutral wind, temperature, composition, atmospheric and ionospheric density distributions as well as make in-situ measurements of the ion motion. NICE uses flight-tested science instruments in a low-inclination orbit where the geometry magnetically links the in-situ and remote sensing measurements. NICE instruments include a visible dual wavelength two directional viewing Fabry-Perot Doppler interferometer, a one dimensional Extreme Ultraviolet Violet (EUV) altitude profiler, a Far Ultra-Violet (FUV) 2di Imager (135.6 nm (OI) and 155 nm LBH) and an Ion Velocity Meter (IVM) consisting of a drift meter and a retarding potential analyzer.

ITIT-09 Modeling Ionospheric Effects for the LWA - by Christopher Watts

Status of First Author: Non-student

Authors: Christopher Watts, Masaya Kuniyoshi, LWA Team

Abstract: The Long Wavelength Array (LWA) is a new telescope/interferometer facility being established to do astrophysical observations in the frequency range 10 MHz to 90 MHz. As such, measurements will be strongly affected by the ionosphere. In fact, part of the LWA mandate is to make highly precise measurements of the ionosphere. We present here preliminary modeling results of the effect of the ionosphere on the LWA for a single station beam. As expected, detrimental effects of a non-uniform ionosphere are most severe at lower frequency/longer wavelength. Beam divergences of as much as ± 5 degrees are to be expected.

ITIT-10 The Combined Radio Interferometry and COSMIC Experiment in Tomography (CRICKET) Campaign - by K. F. Dymond, presented by L. J Rickard

Status of First Author: Non-student

Authors: K. F. Dymond(1), C. Watts(2), C. Coker(1), P. Bernhardt(1), N. Kassim(1), J. Lazio(1), A. Cohen(1), K. Weiler(1), P. Crane(1), L. J Rickard(3), G. Taylor(4), F. Schinzel(4), Y. Philstrom(4), S. Close(5), P. Colestock(5), S. Myers(6), A. Dhatta(6)

Affiliations:

- 1) Naval Research Laboratory, Washington, DC
- 2) Department of Electrical and Computer Engineering, University of New Mexico, Albuquerque, NM
- 3) Long Wavelength Array Project, University of New Mexico, Albuquerque, NM
- 4) Department of Physics and Astronomy, University of New Mexico, Albuquerque, NM
- 5) Los Alamos National Laboratory, Santa Fe, NM
- 6) National Radio Astronomy Observatory, Socorro, NM

Abstract: The Combined Radio Interferometry and COSMIC Experiment in Tomography (CRICKET), carried out in September 2007, combined 74 MHz observations by the Very Large Array (VLA) of background radio sources, with beacon receiver measurements of the COSMIC satellite constellation. Its primary goal was to attempt 3-D tomography over the VLA, to correlate to integrated delta-TEC measurements derived from the 74 MHz phase data, and to tie this to global ionospheric structure determined by the COSMIC/FORMOSAT-3 satellites. During the campaign we were fortunate to catch a Mid-Scale Traveling Ionospheric Disturbance (TID) moving across the VLA site, and observed its effects in the VLA data, the COSMIC data, and in ground-based GPS data. As a result, we were able to characterize the electron density distribution, speed, wavelength and period of the TID. The VLA data provide a glimpse into the ionospheric information that can be derived from future low-frequency radio interferometers, such as the Long Wavelength Array.

ITIT-11 Principles of Dynasonde Data Acquisition and Processing - by Nick Zabotin

Status of First Author: Non-student

Authors: N.A. Zabotin (Univ. of Colorado at Boulder; Dynasonde Solutions Ltd.; nikolay.zabotin@colorado.edu), J.W. Wright (Dynasonde Solutions Ltd.; billwrightster@gmail.com)

Abstract: Dynasonde principles have been developed continuously for more than 30 years, and now they comprise quite an elaborate and beautiful concept. Unique dynasonde products include: phase-based echo recognition, echo classification into traces, autonomous scaling of ionospheric parameters, 3-D plasma density inversion (NeXtYZ), small-scale irregularity diagnostics, and vector velocities, all obtained directly from ionogram data. Dynasonde 21 is a comprehensive software suite that integrates all of the dynasonde data analysis methods. We describe features of dynasonde ideology implemented in Dynasonde 21 and its most recent successful application, with the new 8-channel fully digital HF Radar (built by Scion Associates Inc.), at NASA's Wallops Flight Facility.

**ITIT-12 Spatial Effects of Multiple Scattering of HF Signals in the Ionosphere: Theory and Experiment
by Nick Zabotin**

Status of First Author: Non-student

Authors: Nikolay Zabotin (Univ. of Colorado at Boulder; Dynasonde Solutions Ltd.; nikolay.zabotin@colorado.edu), Albin Gasiewski (Univ. of Colorado at Boulder; Al.Gasiewski@colorado.edu), J. William Wright (Dynasonde Solutions Ltd.; billwrightster@gmail.com), Gennady Zhabankov (Inst. of Physics, Southern Federal Univ., Russia; zhabankov@ip.rsu.ru)

Abstract: The theory of multiple scattering of MF/HF radio waves by intermediate-scale (0.1-2 km) ionospheric irregularities in the course of near-normal incidence reflection, as developed earlier by the authors, predicts significant reduction of the integral intensity of a signal reflected from the ionosphere in the vicinity of a ground-based transmitter (several tens of kilometers), followed by an enhancement at a greater distance. This effect is measurable using pulsed radar signals and a mobile setup comprising a digital receiver, a controlling laptop computer, and a GPS receiver. We report the first results of the experiment and of a related theoretical development.

ITIT-13 Observing the coupling of ionospheric irregularities and thermospheric neutral dynamics using Fabry-Perot observatories: a new approach - by Shaun Armstrong

Status of First Author: Student NOT in poster competition Masters

Authors: Shaun Armstrong (sjaarmstr@uiuc.edu), Jonathan Makela (jmakela@uiuc.edu), John Meriwether (john.meriwether@ces.clemson.edu)

Abstract: The RENOIR experiment involving two Fabry-Perot interferometers (MiniME FPI) and an all-sky imaging system as well as GPS differential receivers is planned for deployment during this coming summer to the Cape Verde islands in the African sector as part of the NASA-funded contributions to the International Heliospherical Year (IHY). From the FPI data, we will study how neutral dynamics affect the development of ionospheric irregularities (depletions). The two FPI systems will be used in a bistatic mode to measure the thermospheric zonal and meridional neutral wind components and the neutral temperature in the common volume region established by overlapping line-of-sight views of the 630-nm nightglow. The two FPI systems will be used at two Cape Verde sites separated by ~300 km to also study the wind gradients and gravity waves known to be present in the thermosphere. The RENOIR instruments will study the thermosphere-ionosphere coupling during the passage of equatorial plasma bubbles (EPB) as well as the possible effects of the background neutral wind field on the development of EPBs. The poster presents current results from the two MiniME FPI systems during their pre-deployment testing phase and discusses the technique developed for multi-ring analysis of the MiniME data.

ITIT-14 Recent Upgrades to the Kodiak Island SuperDARN Radar - by Richard Todd Parris

Status of First Author: Student NOT in poster competition PhD

Authors: R. T. Parris, W. A. Bristow, S. Sun, Geophysical Institute, University of Alaska Fairbanks

Abstract: Recent upgrades to the Kodiak SuperDARN radar include DDS up-converters, imaging digital receivers, GPS synchronization, and a new timing signal generator. The details of these systems is presented, along with first observations.

ITIT-15 Enhanced Line of Sight Velocity Analysis Using an Aperiodic Pulse Sequence on the Kodiak and King Salmon Radars - by Jeffrey Spaleta

Status of First Author: Non-student PhD

Authors: J. Spaleta, W. Bristow, R. T. Parris, M. Balaji, S. Watari

Abstract: A previously developed 16 pulse sequence was recently tested on both the Kodiak and King Salmon SuperDARN radars. The resulting autocorrelation function (ACF) for this pulse sequence consists of 121 unique, aperiodically spaced lags. The large number of unique lags makes it possible to use aperiodic spectral analysis techniques, such as the Lomb periodogram, to construct an ACF spectrum. Using such a technique, ionospheric backscatter line of sight velocities can be extracted from ranges known to

be contaminated by strong ground scatter. The currently implemented FITACF algorithm makes a strict assumption concerning the existence of a single dominant frequency component in the ACF. Thus, the FITACF algorithm is not reliable when multiple strong velocity components are present in the scattering volume, nor can it discern ionospheric backscatter when strong backscatter is dominant. This poster focuses on a comparison of the line of sight analysis of the aperiodic 16 pulse sequence using both the traditional FITACF algorithm as well as aperiodic spectral analysis techniques. The analysis of several examples of multiple velocity component situations will be presented. It will be argued that the 16 pulse sequence can be used in place of the traditional 8 pulse sequence without significantly disrupting the existing FITACF line of sight velocity data products. Furthermore, the 16 pulse sequence raw samples or rawacf information can be processed off-line to identify occurrences of multi-mode backscatter to supplement FITACF fitted velocity data.

Long-Term Variations of the Upper Atmosphere

LTRV-01 Solar cycles and geomagnetic variability of nighttime topside hydrogen, oxygen and helium ion fractions over Arecibo - by Christiano Garnett Marques Brum

Status of First Author: Non-student PhD

Authors: Sixto Gonzalez, Nestor Aponte, Diana Prado Garzon

Abstract: In this work we are comparing incoherent scatter radar data of the H⁺, He⁺ and O⁺ fractions for the months of June solstice (May, June, July and August) from two years (1998 and 2000) with solar flux and geomagnetic variations. Due to the strait dependence of the response of the ion fractions with the solar and geomagnetic variations, we isolated the real contribution of these parameters by local time and altitude as variation rates. Previous results demonstrate that at the altitude range in study (350 to 1250km) there is a positive (negative) responses of the ion O⁺ (H⁺) with the variation of solar flux while the dependence of the He⁺ rates presented three different behaviors in altitude dependents of time, i.e., detected two regions of behavior inversion. We also found evidences of the formation of a small layer of the He⁺ son after the local midnight in altitudes around 875km with increased geomagnetic activity. A strong dependence with geomagnetic variation was detected for the ions of H and O post midnight generating two layers. However, these layers were detected in different altitude's far from each other at 340km.

LTRV-02 Solar, geomagnetic and seasonal variability of the NmF2 and foF2 over Arecibo Observatory – by Eva Robles, presented by Ethan Engle

Status of First Author: Non-student

Authors: Ethan Engle, Christiano Brum, Craig Tepley, Sixto González, Pedrina Terra Santos

Abstract: We are analyzing the electronic density (NmF2) in the F region critical frequency (foF2) and peak height (hmF2) obtained from a bottom side incoherent scatter radar data of 268 days (142 experiments) recorded at Arecibo Observatory (18.35oN, 66.75oW - 46.7o dip angles) between 1985 and 2005. In order to study its variability with solar and geomagnetic activity we are comparing with decimetric solar flux (F10.7cm) and kp indexes. Previous results show different responses of the NmF2 and foF2 with F10.7cm and kp index variation for equinox, summer and winter seasons. The results obtained in this work will be compared with previous results of the neutral winds.

LTRV-03 The long-term changes in the red 630.0 nm line nightglow intensity as an indicator of the dynamical changes in the upper atmosphere and decrease in the neutral gas density - by Goderdzi Didebulidze, presented by Nikoloz Gudadze

Status of First Author: Non-student

Authors: G. G. Didebulidze, N. B. Gudadze, L. N. Lomidze, G. Javakhishvili, Georgian National Astrophysical Observatory, Ilia Chavchavadze State University, Tbilisi, Georgia (guda@genao.org)

Abstract: The long-term variations in the red 630.0 nm line intensity are investigated using Abastumani (41.75 N; 42.82 E) photometrical data obtained in 1957-1993, and the ionosphere F2 layer data at Tbilisi (41.65 N, 44.75 E) ionosonde station (1963-1986). The long-term increase in the red line intensity, observed after astronomical twilight for most seasons and its decrease near midnight is considered as a result of the lowering of the ionosphere hmF2 peak height. Our theoretical simulation shows that the

different values of the long-term change in the red line intensity (positive trend after twilight and negative near midnight) in different seasons may result from the long-term decrease in the southward wind velocity (or increase in the northward wind velocity) and the decrease in neutral density in these regions. An estimation of the lowering of the ionosphere peak height and corresponding red line intensity nighttime behavior is done by using a Chapman type (damping in time) layer for the ionosphere F2 region electron density height distribution, which is solution of ambipolar diffusion equation and takes into account a meridional wind velocity. A decrease in the thermosphere neutral density by about 10% over the 37 years period is consistent with the observational results.

The preliminary results of nightglow intensity of the H α (656.3 nm) line (obtained at Abastumani in 1958-1987) also shows of its negative trend, which could be connected to a decrease in the total hydrogen content in the geocorona.

LTRV-04 Investigation of Solar Cyclic and Climatic Influences on Geocoronal Hydrogen - by Susan M Nossal

Status of First Author: Non-student

Authors: Nossal, S.M., E.J. Mierkiewicz, F.L. Roesler, L.M. Haffner, R.J. Reynolds, R.C. Woodward, nossal@physics.wisc.edu

Abstract: The investigation of natural variability and climate change in the upper atmosphere requires accurate long-term data sets. Our geocoronal hydrogen emission data is now of sufficient extent and precision to investigate solar cyclic trends and to begin to examine possible climatic changes. These data have been acquired with similarly designed ground-based Fabry-Perot Interferometers located in Wisconsin and Arizona. High signal-to-noise observations over solar cycle 23 taken with the Wisconsin H-alpha Mapper Fabry-Perot (WHAM) have quantified a statistically significant solar cyclic influence on the geocoronal hydrogen column emission intensity. The ratio between solar maximum and minimum column emission intensities is close to 1.5. Observations taken by WHAM during solar minimum conditions in 1997 and 2006 agree with observations taken during solar minimum conditions in 1985 with the "pre-WHAM" Fabry-Perot to within 15% over most of the shadow altitude range. These data establish a reference data set of highly precise, consistently calibrated, thermospheric + exospheric hydrogen column emission observations that can be used to compare with future observations. In this poster, we will discuss the Wisconsin long-term data set as well as plans for modeling studies to investigate the magnitude of predicted solar cyclic and climatic changes in thermospheric hydrogen over the 30-year period of the Wisconsin long-term mid-latitude data set.

LTRV-05 H-alpha Observations using Arecibo's new low resolution FPI - by John Noto

Status of First Author: Non-student

Authors: John Noto, P. Terra, M. Migliozi, R. Garcia, E. Robles, J. Riccobono, R.B. Kerr

Abstract: The low resolution single etalon Fabry-Perot interferometer (FPI) in the Optical Laboratory at the Arecibo Observatory has been upgraded to permit remote operation, to improve FPI sensitivity, and to permit FPI response in the near infrared. Integration of a 2048 x 2048 Andor CCD array into the existing low-resolution Fabry Perot Interferometer with a new optical system is complete. Configured with a spectral resolution of 0.0086 nm at 656.3 nm, the low resolution FPI sampled the geocoronal Balmer-alpha emission for sixty nights during new moon periods from September 2006 to September 2007. These observation campaigns were conducted using the new remote control capability in addition to onsite personnel. The single etalon FPI produces multiple orders at the CCD plane corresponding to a full field-of-view of 0.92 degrees. The FPI Hadinger ring pattern is summed annularly, and the three orders are subsequently summed, producing an instrument sensitivity that is 43 times better than the previous single channel photomultiplier detection system. Raw detector response is corrected using both linear (chip bias) and non-linear techniques (flat-field) prior to ring-summing. A frequency stabilized HeNe laser at 632.8 nm is used to establish the FPI response function. Effective exospheric temperature and line profile asymmetries determined after decomposition of the instrument response function from the measured airglow emission are presented. Identification and climatological characterization of non-Maxwellian H distributions, with simultaneous quantification of H $^+$ abundance and flow in the topside ionosphere by the Arecibo incoherent scatter radar, are measurements central to our goal of improved understanding of H on H $^+$ charge exchange escape of H.

LTRV-06 Solar Wind Structure Sources and Periodicities of Global Electron Hemispheric Power over Three Solar Cycles - by Barbara Emery

Status of First Author: Non-student

Authors: Barbara A. Emery (HAO/NCAR, emery@ucar.edu), Ian G. Richardson, (ian.g.richardson@nasa.gov), David S. Evans (SEC/NOAA, david.s.evans@noaa.gov), and Frederick J. Rich (Lincoln Labs/MIT, frederick.rich@ll.mit.edu)

Abstract: We assess the contributions of various types of solar wind structures (transients, coronal hole high-speed streams (HSS), and slow speed wind) to hourly average global electron hemispheric power (Hpeg). The time variation of the solar wind velocity (Vsw) and Hpeg are determined by HSSs, which contribute ~47% to the total Vsw and ~46% to the total Hpeg. Transients, or Coronal Mass Ejections (CMEs), contribute ~42% of Hpeg in solar maxima, and ~7% in solar minimum, but account for most of the magnetic storm behavior because they are associated with large magnitudes of the IMF B field. Cross-correlations of hourly Hpeg that lag hourly Vsw*Bz by 1 hour for negative Bz are approximately -0.6 for all solar wind structures. Hpeg exhibits solar rotational periodicities similar to those for Vsw using both Lomb and FFT analyses, where the 7 and 9-day periodicities are particularly strong in the present solar minimum (starting February 2006). Periodicities longer than 100 days can be different for different solar structures, and not as well correlated between Vsw and Hpeg. The 'semiannual' (183+/-17 days) periodicity in auroral indices is largest in equinoxes because of the preferred solar wind entry during equinoxes. Such an equinoctial maximum is also found in the 'auroral index' of Hpeg over most of the three solar cycles. A strong 'semiannual' periodicity in Vsw maximizing in equinoxes was also found in the late 1990s around solar minimum, which enhanced the equinoctial maximums found in Hpeg. When the 'semiannual' periodicity in Vsw does not maximize in equinoxes, such as during the declining phase from solar maximum from July 2002 to January 2006, the equinoctial 'semiannual' periodicity in Hpeg was very small

Solar Terrestrial Interactions in the Upper Atmosphere

SOLA-01 Extending F10.7's Time Resolution to Capture Solar Flare Phenomena - by Ariel Acebal

Status of First Author: Student IN poster competition PhD

Authors: Ariel Acebal

Abstract: Solar ultraviolet (UV) radiation ionizes the neutral components in the atmosphere, which is partly responsible for the formation of the ionosphere and contributes to heating of the upper atmosphere. Solar flares change key parts of the solar spectrum at times by several orders of magnitude. These changes modify the Earth's upper atmosphere, causing problems to communication systems and space operations such as increased satellite drag. Unfortunately, solar UV measurements can only be observed with space-based sensors. In order to work around this limitation, the solar radio emissions at a wavelength of 10.7 cm have been used as a proxy for the solar UV radiation. This measurement, known as the F10.7 index, is a daily snapshot of the solar activity at the time it is taken and does not capture the changes, such as flares, that occur throughout the day. In order to capture this daily variation, we used 1-second cadence solar radio data and compared it to solar UV measurements taken once per orbit by the TIMED satellite. As expected, we found significant correlations between some radio frequencies and different UV wavelengths during quiet times. These results showed correlation values of 0.80 or better and were similar to F10.7/UV correlations results from previous studies. During solar flares, the highest correlation values shifted to a higher radio frequency for the lower UV wavelengths. This provides promise for a radio-based solar UV proxy that contains solar flare contributions.

SOLA-02 Deriving Neutral Winds from Global 4-D Electron Density Fields - by Seebany Datta-Barua

Status of First Author: Non-student

Authors: Seebany Datta-Barua, Gary Bust, Geoff Crowley, and Natalie Curtis -- Atmospheric and Space Technology Research Associates

Abstract: Several active areas of ionospheric research, such as storm-enhanced densities, require knowledge of physical drivers. Ideally, we would like to have direct global measurements of the winds, E-fields, composition, and temperatures: the drivers of the ion continuity equation. However, in practice, there are so few ground-based instruments and satellites measuring these parameters that knowledge of the drivers is usually missing. On the other hand, the ready availability of ground-based GPS total electron content (TEC) and other ionospheric data has allowed imaging algorithms such as the Ionospheric Data Assimilation

Three-Dimensional (IDA4D) [Bust et al., 2000, 2004] to routinely obtain images of the global electron density field, with spatial resolution of 100 kilometers horizontally and 20 kilometers vertically. We investigate whether these images can be inverted to provide information about the physical drivers such as winds.

We are developing a new inversion algorithm, based on 4D images of global electron density, to estimate the neutral wind ionospheric driver when direct measurement is not available. We begin with a model of the electron continuity equation that includes production and loss rate estimates, as well as ExB drift and diffusion effects. We use ion, electron, and neutral species temperatures and neutral densities from the Thermosphere-Ionosphere Mesosphere Electrodynamics General Circulation Model (TIMEGCM) for estimating the magnitude of these effects. We then model the neutral wind as a power series at a given longitude for a range of latitudes and altitudes. As a test of our algorithm, we have input TIMEGCM electron densities to our algorithm. The model of the neutral wind is computed at 15-minute intervals and validated by comparing to the “true” TIMEGCM neutral wind fields.

We show results for a storm day: 10 November 2004. The agreement between the winds derived from IDA4D versus TIMEGCM “true” winds appears to be time-dependent for the day under consideration. This may indicate that the diurnal variation in certain driving processes impacts the accuracy of our neutral wind model. Despite the potential temporal and spatial limits on accuracy, estimating neutral wind speed from measured electron density fields provided by IDA4D via our algorithm shows great promise as a complement to the more sparse radar and satellite measurements.

SOLA-03 Properties of the Ionospheric Signature of the Low-latitude Boundary Layer During Periods of Southward IMF - by Kelly Ann Drake

Status of First Author: Student NOT in poster competition PhD

Authors: K. A. Drake, U.S.A.F. Academy, dr.kelly@physics.org, R. A. Heelis, U.T. Dallas, heelis@utdallas.edu

Abstract: A study of the behavior of the low-latitude boundary layer is conducted from signatures of the precipitating electrons and the ionospheric convection velocity made in the ionosphere. The observations are made under southward IMF conditions in a highly dynamic environment where temporal changes produce large excursions in the location of both the convection reversal boundary and the poleward edge of the particle precipitation that is associated with the outer edge of the low-latitude boundary layer. We describe the latitudinal width of the boundary layer as the displacement between these boundaries and the convection reversal boundary. On either side of local noon we find the boundary layer has a latitudinal extent of one to two degrees near dawn and dusk. The potential across the boundary layer increases toward local noon and accounts for no more than 30% of the potential across the polar cap derived from direct connection with the solar wind. The boundary layer is wider on the dusk side than on the dawn side, but the average potential across the dawn-side boundary layer is larger than that across the dusk-side layer. The resulting electric field across the dawn-side layer is approximately twice that found in the dusk-side layer. We find a higher level of variability in the boundary layer width and potential on the dawn side that may be related to higher levels of turbulence and wave activity allowed by the orientation of the IMF with respect to the bow shock.

SOLA-04 Periodic Modulation of the Thermosphere by Solar Wind - by Jiuhou Lei

Status of First Author: Non-student PhD

Authors: Jiuhou Lei, Jeffrey P. Thayer, Jeffrey M. Forbes, Eric K. Sutton, R. Steven Nerem. Aerospace Engineering Sciences Department, University of Colorado, Boulder, Manuela Temmer, Astrid M. Veronig, Institute of Physics, University of Graz, Graz, Austria

Abstract: Thermosphere densities at 400 km altitude from accelerometer measurements on the CHAMP satellite are used to investigate oscillations at periods < 11 days during the declining phase of solar cycle 23 (2002-2007). Density spectra reveal the presence of prominent periods around 5 days, 7 days and 9 days. Specifically, a pronounced 9-day periodicity is obtained in the years from 2004 to 2007, and a strong periodicity of about 7 days occurred in 2006 and 2007. The 5-day periodic oscillations were also seen during 2004-2007, but their powers are smaller than those of 7-day or 9-day oscillations. These periodic oscillations in neutral density tend to occur during the latter part of the declining solar cycle when periodic fast streams in the solar wind modulate the level of geomagnetic activity in the geospace environment. In fact, the periodic oscillations seen in neutral densities are simultaneously present in the solar wind and geomagnetic activity index K_p , whereas not in either the 10.7 cm solar radio flux or in the TIMED/SEE solar EUV irradiance data. The periods of 5, 7 and 9 days apparently reflect subharmonics of the 27-day rotation, and may be related to the longitudinal distribution of coronal holes. The periodic oscillations in neutral density are felt

globally, and are proportional to the periodic Kp perturbations at the same frequency. The neutral density data thus suggest that these oscillations are related to the solar wind, and not to the influences of planetary waves at similar periods originating in the lower atmosphere.

SOLA-05 Local time dependence of the prompt ionospheric response for the November 2004 superstorms
by Anthony Mannucci

Status of First Author: Non-student

Authors: Anthony J. Mannucci, JPL/Caltech, Bruce T. Tsurutani, JPL/Caltech, Michael C. Kelley, Cornell University. Byron A. Iijima, JPL/Caltech, Attila Komjathy, JPL/Caltech

Abstract: The global nature of prompt penetrating electric fields suggests that specific local time dependencies should exist. The east-west orientation of the undershielded zonal electric field at low latitudes should be reversed between day and night for an observer on Earth. Dawn-dusk directed electric fields during daytime lead to plasma uplift and the “dayside superfountain” increasing the total electron content (TEC) of the ionosphere at low to middle latitudes by a factor of ten or more for intense storms. In the midnight sector, the penetration electric field orientation should lead to plasma downdraft. In contrast to daytime, the nighttime ionospheric response to penetration electric fields is more variable. Prompt storm-time effects have been studied previously in a limited number of longitude/local time sectors, but no systematic study exists during positive phase storms over a wide range of sectors. We will focus attention on the local time dependence of TEC changes during the November 2004 superstorms, which are known to include a positive storm phase on the dayside. We will use data from the globally distributed network of ground-based GPS receivers and ionospheric data from the GPS receiver onboard the CHAMP satellite that measures total electron content above the satellite altitude of approximately 400 km. The global distribution of the ground receivers, and fixed local time of the satellite orbit are used to isolate and examine local time dependencies of the ionospheric response during the storm period. We find a highly variable local time response for the three major storm events in the November 7-10, 2004 period. Our approach complements detailed observations from radar that are fixed to specific locations on Earth for which the local time is changing.

SOLA-06 GPS and Solar Radio Burst Forensics - by Brady O'Hanlon

Status of First Author: Student IN poster competition PhD

Authors: P. M. Kintner, P.M.S. Kintner

Abstract: On December 6, 2006 a solar radio burst associated with a class X6 solar flare demonstrated that GPS receiver operation is measurably affected by solar radio burst noise at 1.2 GHz and 1.6 GHz. These results were confirmed by observations of two more solar radio bursts over the next eight days. Using these results, the intensities of past solar radio bursts are inferred through analysis of GPS receiver signal strength and, where applicable, compared to existing measurements of those solar radio bursts. The question of whether archived GPS data can be used to detect solar radio bursts in the more distant past as a form of GPS/solar radio burst forensics is addressed in this poster.

SOLA-07 Modeling the thermospheric response to solar flares - by David Pawlowski

Status of First Author: Student IN poster competition PhD

Authors: David J. Pawlowski, University of Michigan dpawlows@umich.edu, Aaron J. Ridley

Abstract: The Global Ionosphere-Thermosphere Model (GITM) is used to simulate the response of the thermosphere to two strong solar flares. Solar EUV data from the SEE instrument onboard TIMED is used as a solar driver during the October 28, 2003 and November 6, 2004 X-class flares, and the resulting perturbed global thermosphere is studied. Data from the accelerometers onboard the Champ satellite are used to compare the model to data. Using the model, the resulting gravity wave during the October 28 flare is also studied.

SOLA-08 Thermospheric and Ionospheric Response to Solar Flare Events - by Liying Qian

Status of First Author: Non-student

Authors: Liying Qian, Stanley C. Solomon, W. Kent Tobiska, Jiuhou Lei

Abstract: Solar X-ray can increase several orders of magnitude during a flare event and trigger significant changes in both the neutral atmosphere and the ionosphere. The NCAR Thermosphere-Ionosphere-Electrodynamics General Circulation Model (TIE-GCM) will be employed to investigate the atmospheric response to several X-class flare events with intensities ranging from X3 to X17. Solar flare spectra will be provided by the SOLARFLARE model developed by the Space Environment Technology. Model simulated neutral density and TEC enhancements will be compared to CHAMP satellite (CHAllenging Minisatellite Payload) measurements to examine thermospheric and ionospheric response to the selected X-class flare events.

SOLA-09 Altitude Dependence of Thermospheric Winds in HWM07 - by Kate Roach

Status of First Author: Student IN poster competition Undergraduate

Authors: K.A. Roach(1), D.P. Drob(1), J.T. Emmert(1), G. Crowley(2), S.E. McDonald(1)

(1) Space Science Division, US Naval Research Laboratory, 4555 Overlook Ave. SW, Washington, DC 20375

(2) Atmospheric and Space Technology Research Associates (ASTRA), 11118 Quail Pass, San Antonio, TX, 78249

Abstract: Historically, neutral winds in the thermosphere have been assumed to be constant with altitude above ~250 km because of a lack of observational data. However, but it is known that increased solar irradiance can increase the amount of ion drag in the thermosphere, the effect of which can dominate over the molecular viscosity that smoothes out vertical gradients. Thus, the height at which winds become independent of altitude can vary with solar conditions. We compare the new Horizontal Wind Model (HWM07) to a first-principles physics model (TIME-GCM) and data at different latitudes at solar minimum and maximum to examine the extent to which HWM07 models vertical gradients in the upper thermospheric winds.

SOLA-10 Latitudinal Response of Thermosphere Density to High-Latitude Heating - by Eric K Sutton

Status of First Author: Non-student PhD

Authors: E K Sutton, J M Forbes, J P Thayer, D J Knipp

Abstract: A series of three geomagnetic storms occurred during the period of 20-29 July, 2004, each with unique characteristics of energy input, which affords the opportunity to observe response characteristics of the thermosphere. By studying these storms in such close vicinity to one another, the aliasing effects of satellite sampling, seasonal and solar cycle variations are mitigated. Total mass density from the CHAMP satellite near 400km altitude is used to define the response time of the thermosphere to the high-latitude heating source. Differences between the day and night time density response at all latitudes is discussed in the context of the various mechanisms. Generally, response times are between 1.5-2.5 hours when most of the response can be attributed to changes in meridional circulation. During the night, spikes can occur in the response time which can be related to traveling atmospheric disturbances. Currently, empirical models cannot represent the individual mechanisms for energy propagation. This paper serves as a preliminary study to qualitatively and quantitatively define the spatial response due to several of these mechanisms. Efforts will be made to include the entire span of the density dataset, 2001-2007, increasing the statistical integrity of the study.

SOLA-11 Storm-Time Comparisons of CMIT Results with GPS Data - by Wenbin Wang

Status of First Author: Non-student

Authors: Wenbin Wang, Jiuhou Lei, Alan Burns, Stanley C. Solomon, Harlan Spence and Mike Wiltberger

Abstract: CMIT 2 has been run for three geomagnetic storms to analyze model performance during these different events. The analyses shown here are comparisons between the modeled TEC and ground based TEC changes for the initial phase of these events and comparisons between modeled O/N2 and GUVI data throughout the events. Despite the nature of the three storms varying greatly, CMIT was able to simulate the TEC variations in the initial phase of the storms. Later parts of the storm

presented a greater challenge. The neutral composition variations were also reproduced well in the initial phase of the storm as they were, for the most part, in the main phase, but there were significant differences between CMIT and GUVI data in the recovery period.

SOLA-12 Fluorescence and Photodissociation of Nitric Oxide near 191 nm - by Justin D. Yonker

Status of First Author: Student IN poster competition PhD

Authors: Scott M. Bailey, Virginia Tech, scott.m.bailey@vt.edu. Larry J. Paxton Johns Hopkins Applied Physics Lab
Larry.Paxton@jhuapl.edu

Abstract: It is well known that the nitric oxide (NO) fundamental vibration at 5.3 microns is crucial to the thermal budget of the lower thermosphere (LT). The energy balance in the LT thus depends on the overall NO abundance which, in the sunlit thermosphere, is particularly sensitive to the NO photodissociation rate, the threshold for which is near 191 nm. Just below this energy lies the origin of the NO delta bands. This band is defined by the electronic transition from the ground X ($v''=0$) state to the perturbed C ($v'=0$)/B ($v'=7$) state. Because the dissociation limit lies just above the band origin, both the photodissociation and fluorescence rates are sensitive to the rotational levels of the C/B state. Four relaxation channels are possible from the C/B state: UV fluorescence to the X state, IR emission to the A state, predissociation to the a state continuum, and quenching. In this paper branching ratios for these competing processes are used to calculate the rotational emission rate factor (i.e. g factor) which is then used to model the NO delta band fluorescence spectrum. To obtain the NO abundance from observed delta band emissions the contribution of the preassociative $N+O \rightarrow NO(C/B) \rightarrow NO(X)+h\nu$ (191 nm) reaction must also be considered.

SOLA-13 Particle-In-Cell Simulation of Naturally Enhanced Ion Acoustic Lines Produced by an Electron Beam - by Marcos Diaz

Status of First Author: Student IN poster competition PhD

Authors: Marcos Diaz (Boston University), Meers Oppenheim (Boston University), Joshua Semeter (Boston University), Matt Zettergren (Boston University)

Abstract: A Particle-In-Cell (PIC) approach is presented and utilized to simulate Naturally Enhanced Ion Acoustic Lines (NEIAL). In particular, a 1D simulation is performed of a small F-region plasma volume to study the effect of Langmuir turbulence on the Incoherent Scatter Radar (ISR) spectra. The effect of the electron beam parameters over the ISR are studied for multiple radar wave numbers.

Polar Aeronomy

POLA-01 High-resolution PFISR observations of NEIALs and associated auroral fine structures - by Robert Michell

Status of First Author: Student NOT in poster competition PhD

Authors: Marilia Samara, Southwest Research Institute

Abstract: We present results from a coordinated campaign of common-volume optical and PFISR observations, during February and March of 2008. Several Naturally Enhanced Ion Acoustic Lines (NEIAL)s were observed, while the specific radar mode allowed for maximum time resolution (12 millisecond) raw data along the field-aligned direction. These data indicate that the enhanced returns occur during very short time intervals (< 1 second) and high resolution (33 millisecond) auroral imaging reveals that their occurrence is associated with specific types of auroral fine structures. The features of both the auroral structures and associated NEIALs will be investigated, with the intent of gaining insight into possible NEIAL generation mechanisms.

POLA-02 New results from the Poker Flat all-sky imaging Fabry-Perot spectrometer - by Mark Conde

Status of First Author: Non-student

Authors: Mark G. Conde, University of Alaska Fairbanks, Callum Anderson, LaTrobe University (Australia), Carl Anderson, University of Alaska Fairbanks

Abstract: The all-sky imaging Fabry-Perot spectrometer at Poker Flat has recently been upgraded by replacing its old intensified CCD detector with an electron-multiplying CCD camera. This has yielded a sensitivity gain of several times, relative to the previous system. The instrument control software was also upgraded to a new version, produced by LaTrobe University in Australia. As a result, several new observing modes and capabilities are now available. We will present some preliminary data acquired with the upgraded instrument during the 2008 spring observing season.

POLA-03 Thermospheric Studies in Antarctica Using Fabry-Perot Spectrometers at Mawson and Davis Stations - by Callum Anderson, presented by Mark Conde

Status of First Author: Student NOT in poster competition PhD

Authors: Callum Anderson, LaTrobe University (Australia), Mark G. Conde, University of Alaska Fairbanks, Peter L. Dyson, LaTrobe University (Australia), Theo Davies, LaTrobe University (Australia), M. J. Kosch, University of Lancaster (UK)

Abstract: La Trobe University has recently installed a new all-sky imaging Fabry-Perot spectrometer at Mawson Station, Antarctica. It is capable of recording independent spectra from many tens of locations across the sky simultaneously, from which parameters corresponding to temperature and line-of-sight wind speed are derived. This instrument, in conjunction with La Trobe's existing spectrometer at Davis Station, provides new opportunities for investigating small-scale upper atmospheric dynamics. Initial data are presented from the instrument's first season of operation (2007), and opportunities for common-volume campaigns with Davis are explored.

POLA-04 Preliminary results of wave generation from a local scale thermospheric model - by Shaun L. Cooper, presented by Mark Conde

Status of First Author: Student NOT in poster competition PhD

Authors: Shaun L. Cooper, LaTrobe University (Australia), Mark G. Conde, University of Alaska Fairbanks, Peter L. Dyson, LaTrobe University (Australia)

Abstract: A simplified three dimensional, time-dependant model of a local region of Earth's thermosphere is being developed to investigate dynamical processes occurring over spatial scales of less than 100 km. Because hydrostatic equilibrium is not enforced in the model, it is well suited for studying processes that must be represented with high spatial and temporal resolution, such as wave activity and local upwelling. The model domain currently extends 1000 km zonally, 600 km meridionally and encompasses the 100 to 400 km altitude range. The typical cell size is 20 x 15 x 0.75 km. The model is being used to conduct simple numerical experiments that characterize the thermospheric response to various scenarios of time-dependent energy and momentum deposition. Some initial results will be presented.

POLA-05 Volumetric imaging of the auroral ionosphere - by Thomas Butler

Status of First Author: Student NOT in poster competition PhD

Authors: Thomas Butler, Joshua Semeter, Craig Heinselman, Michael Nicolls, John Kelly, Donald Hampton

Abstract: The Poker Flat Incoherent Scatter Radar (PFISR) is the first dedicated ISR employing an electronically steerable array. We demonstrate the capabilities of PFISR for producing three-dimensional volumetric images of the ionospheric E-region during auroral activity. The volumetric data were acquired using a square array of 11×11 scan angles, covering an angular space of 35×35 degrees. The array was repointed on a pulse-to-pulse basis, with the full set of 121 angles sampled every 0.6 s. A phase-coded pulse was used that provided ~ 1.5 -km range resolution. The output from the demodulator was converted to electron density by applying the Buneman approximation to measurements of backscattered power. The resulting 3D images were

quantitatively compared with all-sky white-light camera observations through an ion continuity calculation, demonstrating good agreement. A practical upper limit to the volumetric imaging frame rate in this mode is ~ 15 Frames/s, which corresponds to 48 pulses per angle, yielding uncertainties of $\sim 14\%$. At this cadence, ionospheric variability within the volume appears to be fully resolved, a result supported both observationally and through a consideration of theoretical ionospheric response times. The efficacy of this mode for addressing time-dependent studies of magnetosphere-ionosphere interactions is discussed.

POLA-06 Storm/Quiet Ratio Comparisons Between TIMED/SABER NO+(v) Volume Emission Rates and Incoherent Scatter Radar Electron Densities at E-Region Altitudes - by Jose R Fernandez

Status of First Author: Non-student PhD

Authors: J. R. Fernandez(1), C. J. Mertens(1), D. Bilitza(2), X. Xu(3), J. M. Russell III(4), and M. G. Mlynczak(1)
(1) NASA Langley Research Center, Hampton, VA USA. (2) George Mason University, Fairfax, VA USA (3) SSAI, Inc., Hampton, VA USA, (4) Hampton University, Hampton, VA USA

Abstract: Broadband infrared limb emission at 4.3 μm is measured by the TIMED/SABER instrument. At night, these emission observations at E-region altitudes are used to derive the so called NO+(v) Volume Emission Rate (VER). NO+(v) VER can be derived by removing the background CO₂(nu₃) 4.3 μm radiance contribution using SABER-based non-LTE radiation transfer models, and by performing a standard Abel inversion on the residual radiance. SABER observations show that NO+(v) VER is significantly enhanced during magnetic storms in accordance with increased ionization of the neutral atmosphere by auroral electron precipitation, followed by vibrational excitation of NO+ (i.e., NO+(v)) from fast exothermic ion-neutral reactions, and prompt infrared emission at 4.3 μm . Due to charge neutrality, the NO+(v) VER enhancements are highly correlated with electron density enhancements, as observed for example by Incoherent Scatter Radar (ISR). In order to characterize the response of the storm-time E-region from both TIMED/SABER and ISR measurements, a Storm/Quiet ratio (SQR) parameter is defined as a function of altitude. For TIMED/SABER, the SQR is the ratio of storm-to-quiet NO+(v) VER. SQR is the storm-to-quiet ratio of electron densities for ISR. In this work, we compare TIMED/SABER and ISR SQR values for different magnetic storm events. Preliminary results indicate a good correlation between TIMED/SABER and ISR SQR values particularly between 100 to 120 km. SQR values are intended to be used as a correction factor to be included in an empirical storm-time correction to the International Reference Ionosphere model at E-region altitudes.

POLA-07 The Velocity Filter Effect Observed in Cusp Proton Aurora - by Jeffrey Morgan Holmes

Status of First Author: Student IN poster competition PhD

Authors: Jeffrey M. Holmes 1, Boris Kozelov 2,3, Andrey S. Kirillov 2, Dag A. Lorentzen 1, Fred Sigernes 1, Charles Deehr 4
1 University Centre in Svalbard (UNIS), Box 156, N-9171 Longyearbyen, Norway.
2 Polar Geophysical Institute, Murmansk region, Apatity, Russia.
3 Institute of Physics and Technology, University of Tromsø, Tromsø, Norway
4 Geophysical Institute, University of Alaska Fairbanks, Fairbanks, AK, USA.

Abstract: Optical ground-based cusp observations of auroral Balmer excited hydrogen emissions at H α (656-nm) and H β (486-nm) were carried out using Ebert-Fastie (E-F) spectrometers during the boreal winter 2006-2007 at Ny-Ålesund (NYA, 76.26N 110.98E geomagnetic) and Longyearbyen, Norway (LYR, 75.31N 111.88E geomagnetic), respectively. The sites are located 118 km apart on a line of roughly constant geomagnetic longitude. An upgraded E-F spectrometer, measuring H α , has been added at LYR, allowing for comparison of H α and H β emissions at the LYR site and variations in H α between LYR and NYA. Analysis of the two emissions from the spectrometers was performed and a statistically significant difference in precipitating proton energy was found between Longyearbyen and Ny-Ålesund for a ~ 1 hour period. This, in combination with negative B_z and antisunward convection lends support to the velocity filter concept.

POLA-08 Multi-instrument observations of dayside auroral emission dynamics at South Pole - by Irfan Azeem

Status of First Author: Non-student

Authors: S. M. I. Azeem¹, D. J. McEwen², and G. G. Sivjee¹

¹Space Physics Research Laboratory, Embry-Riddle Aeronautical University, Daytona Beach, FL.

²University of Saskatchewan, Saskatoon, Saskatchewan, Canada.

Abstract: Dayside Aurora has been continuously (24 hour) monitored from South Pole during six month of polar winter night, from mid April to mid September. Oscillating auroral phenomenon has been observed via a 6-channel photometer scanning along the magnetic meridian towards the magnetic pole and a CCD spectrograph (CCDS) operating in the near-infrared (700nm – 960 nm) region along the local magnetic zenith. In this paper we present the dynamics of 630 nm and 844.6 nm auroral emission lines in the dayside aurora (in the 1200-1800 MLT sector) in response to modulations in the interplanetary magnetic field (IMF). Examination of CCDS and meridian scanning photometer data shows intensification of both the red (630.0 nm) and OI (844.6) line emissions in the cusp region near 1200 MLT accompanied by modulation of the line intensity at a period of 10-25 minutes. The associated IMF disturbance also shows 10-25 minute period pulsations. These observations of red and OI line emissions and IMF pulsations are discussed within the context of magnetosphere-ionosphere (MI) coupling.

POLA-09 Electron Precipitation Parameters and Ionospheric Conductances Inferred From Auroral Images Acquired by the Visible Imaging System (VIS) on the Polar Spacecraft - by Hamed Bekerat

Status of First Author: Non-student

Authors: Hamed Bekerat and John Sigwarth, NASA Goddard Space Flight Center, Greenbelt, MD20771

Abstract:

The Visible Imaging System (VIS) on the polar spacecraft provided time sequences of auroral images at multiple wavelengths that yield information of auroral dynamics on a global scale with a spatial resolution of ~ 20 km and temporal resolution of ~ 1 minute. Time sequences of VIS images in which the aurora was highly dynamic are used to infer global maps for the electron precipitation parameters, energy flux and characteristic energies, and ionospheric conductances. The maps are inferred from the corresponding VIS images using an auroral model (Lumerzheim et al., 1987). The temporal and spatial resolution of the VIS inferred patterns are unprecedented. The inferred patterns are highly structured and vary significantly on a time scale of less than 5 minutes. These patterns can be very beneficial for global physics-based numerical models for the high-latitude ionosphere which previously had to rely on statistical models for the electron precipitation and ionospheric conductance.

POLA-10 Temporal evolution of the reflection height in response to HF heating in the polar ionosphere - by Christopher Fallen

Status of First Author: Student IN poster competition PhD

Authors: Chris Fallen, Arctic Region Supercomputer Center, Geophysical Institute, University of Alaska Fairbanks
Brenton Watkins, Geophysical Institute, University of Alaska Fairbanks

Abstract: A multi-species ion model of the one-dimensional ionosphere was used to simulate heating effects during high-frequency (HF) ionosphere modification experiments. The electron temperature increases for several seconds over a region extending from the HF-interaction region to hundreds of kilometers above the interaction region in the direction of the geomagnetic field. Corresponding increases in the ion temperature over several minutes are also observed. The magnitude and time variation of the temperature perturbations are in approximate agreement with observations. Increasing the plasma temperature in the F region affects the relevant temperature-dependent chemical reaction rate coefficients and increases the ambipolar diffusion coefficient, which can lead to significant modifications of the electron-density altitude profile. Radar observations indicate that the HF-interaction region is located within several kilometers of the reflection height, where the plasma frequency equals the heater transmitter frequency. The plasma frequency is a function of the electron density so the reflection height altitude may change in response to HF heating. Model simulations are used to estimate the velocity and total displacement of the reflection height altitude.

POLA-11 Observations of auroral-region energy dissipation by Joule heating as a function of spatial scale size by
Travis Gaulden

Status of First Author: Student NOT in poster competition PhD

Authors: T. Gaulden¹, M. F. Larsen¹, R.F. Pfaff²
¹Clemson University, Clemson, South Carolina
²NASA/Goddard Space Flight Center, Greenbelt, Maryland

Abstract: The energy input into the auroral region as a result of both precipitating particles and dissipative current heating has important implications in atmospheric chemistry, in neutral dynamics, and in the electrodynamics of the high-latitude region. Electron density, electric field, and neutral wind measurements are essential in calculating the Joule heating due to the fluctuating component of the electric fields. Such measurements were obtained along the trajectory of two rockets launched 12:31 and 12:45 U.T. on January 19, 2007, from the Poker Flat rocket range in Alaska as part of the JOULE II rocket experiment. The measurements were analyzed, along with model-based parameters such as the magnetic field, neutral density, ion composition ratios, and electron temperature, to obtain the energy dissipation rates in the altitude range from 110 to 140 km and compared with previous results.

POLA-12 New Hardy Auroral Flux Model for Driving TIEGCM - by Peichen Lai

Status of First Author: Student IN poster competition PhD

Authors: Peichen Lai, peichen.lai@bc.edu, Chin S. Lin, Chin.Lin@hanscom.af.mil, William J. Burke, William.Burke.ctr@hanscom.af.mil

Abstract: Auroral particle fluxes are important energy inputs for the TIEGCM modeling. Discrepancies between the model inputs and DMSP observations of auroral fluxes are sometimes significant. More than 20 years of DMSP data show that the average precipitating electrons have log-normal rather than Gaussian distributions as generally assumed. Recently Hardy et al. [2007] re-analyzed the DMSP data and produced a new model which calculates probability densities of energy flux and average energy in auroral oval in given any Kp, magnetic local time (MLT) and latitude (\square). Based on the Hardy [2007] model we attempt to develop a new model to act as the energy source for driving TIEGCM. In the analysis we distinguished the most probable values of log energy flux and log average energy into plasma sheet and magnetosheath sources. We then created new formulas for both log energy flux and log average energy as functions of Kp, MLT and \square . In this paper, conductivities and electron density are modeled by TIEGCM using the new auroral flux model. It is found that TIEGCM simulations with the new auroral flux model provide better estimates of the conductivities and thus more accurately represent the influence of energy inputs and heating distributions in the high-latitude region.

POLA-13 Plasma Wave and Particle Observations in a post Substorm Quiet Auroral Ionosphere - by Erik Thomas Lundberg

Status of First Author: Student IN poster competition PhD

Authors: Erik Lundberg (etl22@cornell.edu) and Paul Kintner, Cornell University, Kristina Lynch and Alex Crew Dartmouth College, Marc Lessard and Sarah Jones, University of New Hampshire

Abstract: On Feb 12th, 2007 an auroral sounding rocket, ROPA (Rocket Observations of Pulsating Aurora), was launched from Poker Flat Rocket Range at 12:45 UT into a region of pulsating aurora with an apogee of ~657km. Poleward of the pulsating aurora region, the payload crossed through a quiet auroral ionosphere. In this poster the results of a 12m tip to tip wire boom VLF receiver are presented along with corresponding electron and ion measurements. Over an altitude range of 500km to 657km wave signatures are observed at integer sub-harmonics of the local hydrogen gyrofrequency (ωH^+). Two prominent bands are observed, one at ωH^+ with a bandwidth of ~150 Hz and a second band sharply cutoff at $\frac{1}{4} \omega H^+$. The waves have peak to peak amplitudes of ~2 mV/m and are correlated with ions having energies of ~100eV -500eV.

POLA-14 Influence of Spatial Structure of High-Latitude Joule Heating on Thermospheric Composition
Astrid Maute

Status of First Author: Non-student

Authors: A. Maute and A.D. Richmond

Abstract: Electromagnetic energy transfer from the magnetosphere to the, high-latitude thermosphere occurs over a range of spatial scales. Most of this energy is converted into Joule heating in the thermosphere. Some aspects of the thermospheric response to this energy input, especially the composition, depend nonlinearly on the intensity of the heating, such that intense heating occurring in a small region can produce a greater global-scale thermospheric composition response than the same amount of heat deposited over a broader area, with less peak intensity. We are using a two-dimensional, time-dependent model of thermospheric dynamics to evaluate the net upward transport of thermospheric molecular species (N₂ and O₂) by high-latitude Joule heating. The net transport is also affected by the duration of the heating for a given air parcel, which depends both on the heating duration at a given location, and on the length of time the air parcel remains at that location before being advected away by large-scale winds. We use results from analyzing the characteristic spatial scales of intense Joule heating, derived from electric-and magnetic-field measurements on the Dynamics Explorer-2 spacecraft, and include them in the numerical model. We show that the net upward transport by small-scale heating structures can be simulated by an effective eddy diffusivity that depends on the heating intensity. Parametrizing the effects of intense heating on the mixing is important for global circulation models, which cannot resolve these small spatial scales explicitly.

POLA-15 Resolute Optical Observation Current status and Future Plan - by Qian Wu

Status of First Author: Non-student

Authors: Qian Wu qwu@ucar.edu, HAO/NCAR, S. C. Solomon stans@ucar.edu, HAO/NCAR

Abstract: We will present current status and future plan for Resolute upper atmospheric optical observation.

POLA-16 Optical estimation of auroral ion upflow: A case study - by Matt Zettergren

Status of First Author: Student NOT in poster competition PhD

Authors: M. Zettergren, J. Semeter, P-L. Blelly, G. Sivjee, I. Azeem, H. Gleisner, M. Diaz, O. Witasse

Abstract: The auroral zone ionosphere is an important source region for magnetospheric O⁺. At ionospheric altitudes, pressure increases (ion upflow) move large quantities of plasma into the transition region where ions can be energized to escape velocity (ion outflow). It is necessary to characterize the source of upflowing plasma to the transition region since it may modulate the intensity of ion outflows. Both ISR and low-orbiting satellites routinely perform single-point measurements of upflow, but neither are able to resolve both the temporal variability and the composition of the upflowing plasma. Ionospheric models can provide both plasma composition and dynamics vs. space and time, but the principal drivers of ion upflow (usually precipitating electrons) must be externally imposed on the simulations. In this work we seek to address these issues in via a novel combination of optical remote sensing and ionospheric modeling.

This work presents a technique to estimate the time evolution and composition of upflowing plasma with minimal assumptions about the precipitating electron source. This technique involves two steps: (1) near-infrared spectroscopic observations of the aurora used to estimate the precipitating electron energy distribution and temporal variability (2) The derived precipitation is then used as input to a multi-fluid/kinetic model of the ionosphere (TRANSCAR) to estimate the resulting plasma upflow. This success of this technique is demonstrated by using optical and ISR data from an auroral event occurring over Sondrestrom, Greenland. Estimates for ion upflow (and other plasma parameters) during the event are presented and the dynamic evolution of the ionosphere is examined.

POLA-17 Imaging ionospheric azimuthal flow bursts and the relationship to aurora using PFISR - Shasha Zou

Status of First Author: Student IN poster competition PhD

Authors: Shasha Zou, Larry Lyons, Michael Nicolls, Craig Heinselman, Chih-Ping Wang

Flow bursts within the ionosphere are the ionospheric signatures of flow bursts in the plasma sheet and have been associated with Poleward Boundary Intensifications (PBIs). Some PBIs extend equatorward from the polar cap boundary, where they can be roughly divided into north-south aligned and east-west aligned structures. In this paper, we present two flow burst events observed by the Poker Flat Advanced Modular Incoherent Scatter Radar (PFISR) in the pre-midnight auroral zone on 28 April 2007, one towards the west and the other towards the east. In both cases, enhanced flows lasted for about 8-10 min with peak velocities exceeding 1500 m/s. The concurrently measured electron density showed that the flow bursts occurred in low conductivity regions. However, near the poleward (equatorward) edge of the westward (eastward) flow burst, strong electron density enhancements were observed in the E region, indicating the presence of discrete auroral arcs associated with the flow bursts. Auroral images from the Polar spacecraft were available at the time of the eastward flow burst and they indicate that this burst was associated with an east-west aligned auroral structure that connected at later MLT to a north-south structure. In addition, simultaneous precipitating particle energy spectrum measured by the DMSP F13 satellite reveals that this auroral structure resulted from mono-energetic electron precipitation associated with a significant field-aligned potential drop. These observations show direct evidence of the relationship between flow bursts, field-aligned currents, and auroral intensifications, and suggest that eastward/westward flow bursts are associated with east-west oriented PBI structures that have extended well within the plasma sheet. This is in contrast to the equatorward directed flow that has been previously inferred for PBIs near the polar cap boundary and for north-south auroral structures. This paper illustrates the use of the PFISR radar for studying the magnetosphere-ionosphere coupling of flow bursts.

Midlatitude Ionosphere or Thermosphere

MDIT-01 SHS Observations of O⁺: Initial Results - by Stanley Briczinski

Status of First Author: Non-student PhD

Authors: S.J. Briczinski, E.J. Mierkiewicz, F.L. Roesler and S.M. Nossal, UW-Madison, Madison, WI

Abstract: Investigators at the University of Wisconsin and St. Cloud State University have recently constructed and deployed a new class of interference spectrometer, called the Field-Widened Spatial Heterodyne Spectrometer (FW-SHS). The FW-SHS produces Fizeau fringes by replacing the return mirrors in a Michelson interferometer with diffraction gratings. These fringes are recorded on a position sensitive detector and Fourier transformed to recover the spectrum over a limited spectral range centered at the Littrow wavenumber of the gratings. The FW-SHS combines interferometric and field-widening gains to achieve sensitivities much larger than conventional grating instruments of similar size and resolving power. We present ground-based FW-SHS observations of the terrestrial O⁺ doublet (2D – 4S) emission at 3726 and 3729 Å. These O⁺ emission lines were detected as part of a Galactic O⁺ interstellar medium program underway at the University of Wisconsin's Pine Bluff Observatory.

We present the initial O⁺ FW-SHS observations, believed to be originating in the F region of the ionosphere. The emission intensities are estimated to be in the range of 0.5-1.5 R. The 3729/3726 line intensity ratio is about $0.48 \pm 0.05:1$ for the atmospheric lines compared to about 1.5:1 for the observed interstellar emission. Preliminary analysis indicates that the intensities of the terrestrial O⁺ lines vary together by about a factor of 2 or more over the course of our measurements over any night with no measurable variation in the doublet ratio. We also present a refinement of the FW-SHS spectral calibration using a CeNe lamp with a known emission spectrum. As this terrestrial O⁺ emission is a relatively unstudied phenomenon, we outline the methodology we expect to use to further study this doublet and discuss its importance to the F region of the ionosphere.

MDIT-02 The behavior of the F2 peak ionosphere over the South Pacific at dusk during quiet summer conditions from COSMIC data - by Alan Burns

Status of First Author: Non-student

Authors: A. G. Burns, Z. Zeng, W. Wang, J. Lei, S. C. Solomon, A. D. Richmond, T. L. Killeen, and Y.-H. Kuo
aburns@ucar.edu

Abstract: The six satellite Constellation Observing System for Meteorology, Ionosphere and Climate (COSMIC) mission makes routine ionospheric measurements over the entire globe using occultation techniques. These observations have been used in this study to develop global-scale climate maps of NmF2 and hmf2 during the southern summer). The southern, Equatorial (Appleton) anomaly becomes displaced southward at dusk and, within about an hour, forms the Weddell Sea anomaly. Coincidentally, the height of the F2 peak increases on the northern boundary of this anomaly. This height increase is also displaced southward as the anomaly is displaced southward, suggesting that the electron density increases are associated with the F2 peak rising. As well as being an interesting phenomenon in its own right, this behavior may shed new light on the formation of the Weddell Sea anomaly. No unambiguous explanation for this behavior can be determined from the data presently available.

MDIT-03 Radiation Belt Storm Probes Mission – An IT Community Asset? - by Joseph Grebowsky

Status of First Author: Non-student

Authors: J.M.Grebowsky, D.G.Sibeck/ NASA Goddard Space Flight Center, B. H. Mauk, N. J. Fox /JHU Applied Physics Laboratory

Abstract: NASA's Living With A Star program's Radiation Belt Storm Probes (RBSP) is part of the NASA Geospace Program. The overarching goal of this program is to achieve a balanced, methodical attack on unresolved areas in the Sun-to-Earth coupling physics that have particular relevance to environmental effects on society and human exploration. The Ionosphere Thermosphere Storm Probe (ITSP) mission is an element in the current LWS Geospace program line following RBSP (launch 2012). It is vital that we continue the implementation of the ITSP program using the assets available, including the RBSP mission. The two near-equatorial orbiting RBSP spacecraft will carry instrumentation to measure the inner magnetospheric, plasmaspheric and trough region plasma populations and fields (from $L \sim 1.1$ to 5.8). With the addition of coincident ground-based observations of ionospheric particle populations and fields there is the potential for using the RBSP and ionospheric observations to enhance understanding of magnetospheric – ionospheric coupling processes. Given the baselined RBSP mission, the questions are : How can the IT community contribute to the RBSP science goals? and conversely: Does RBSP provide measurements that will provide useful inputs to IT studies as we await the ITSP mission?

MDIT-04 Mid-latitude nighttime enhancement in F-region electron density from global COSMIC measurements under solar minimum winter condition - by Xiaoli Luan

Status of First Author: Non-student

Authors: Xiaoli Luan, Wenbin Wang, Alan Burns, Stanley C. Solomon, and Jiuhou Lei
High Altitude Observatory, National Center for Atmospheric Research, Boulder, Colorado, USA

Abstract: Ionospheric electron density profiles retrieved from the COSMIC satellites measurements from November 6, 2006 to February 5, 2007 are used to study the ionospheric nighttime electron density enhancements under winter, solar minimum and geomagnetically quiet conditions. In this work, the peak electron densities of F2-layer (NmF2) derived from COSMIC measurements are found to be in reasonably good agreement with ionosonde observations during the night. Then the geographic morphology and local time and altitudinal dependence of nighttime enhancements are investigated at geomagnetic mid-latitudes (MLAT 20-60°) in the northern hemisphere. From COSMIC observations, the enhancements of electron density are evident near the F2-layer peak at most latitudes and longitudes, however, significant variations in the latitudinal dependence of the occurrence times and net magnitudes of the enhancements are found in different regions. The characteristics of enhancements in the North Atlantic Ocean sector are distinctly different from those in the eastern part of the North American sector, and also from those at longitudes from Europe to Asia, in the Pacific Ocean and the western part of the North American sectors. The NCAR-TIEGCM simulations indicate that the longitudinal variations of enhancements at higher mid-latitudes might be related to the neutral composition changes under the influence of neutral winds and neutral temperatures.

MDIT-05 Ionospheric Storms at a Sub-Auroral Location in the Southern Hemisphere - by Clara Narvaez

Status of First Author: Non-student

Authors: Clara Narvaez, Michael Mendillo

Abstract: At east coast US longitudes ($\sim 70^\circ\text{W}$), ionospheric storms have been studied using several techniques to observe the response of the F-layer to geomagnetic activity. These include: (1) total electron content (TEC) data from the Sagamore Hill Observatory in Hamilton (MA), (2) ionosonde data for the maximum electron density of the F-layer (NmF_2) from Wallops Island (VA), (3) incoherent scatter data for electron density profiles $\text{Ne}(h)$ from Millstone Hill (MA), and most recently (4) the GPS network of TEC observing sites throughout North America. All of these methods report a consistent pattern of an initial positive phase that maximizes with a “dusk effect” at sub-auroral latitudes, followed by nighttime depletion signatures of the trough, and then several days of daytime negative phase effects. Such patterns observed in the $L = 2.5 - 3$ regime in the northern hemisphere have not been examined consistently in the southern hemisphere. While such a study would be possible along the $\sim 70^\circ\text{W}$ meridian in the southern hemisphere, the offset of the Earth geomagnetic dipole axis in this longitude sector makes the blend of solar controlled processes (ordered by geographic latitude) and magnetosphere-ionosphere interactions (ordered by geomagnetic latitude) far from comparable. For example, 40°N geographic typically has a geomagnetic latitude of $\sim 52^\circ$ in the northern hemisphere, while the corresponding 40°S geographic corresponds to a magnetic latitude of $\sim 28^\circ$ in the southern hemisphere. Thus, true geophysically-conjugate locations cannot be found for the sub-auroral domain at $\sim 70^\circ\text{W}$.

In the Australian sector ($\sim 130^\circ\text{E}$), however, the dipole tilt results in geophysically-comparable locations to those at $\sim 70^\circ\text{W}$ in the northern hemisphere. We have taken the 75 storm events during solar cycle 20 studied with TEC data by Mendillo and Klobuchar (Radio Sci., 41, RS5S02, doi:10.1029/2005RS003394, 2006) and conducted the same analysis using ionosonde data from Hobart, Tasmania (43°S , 147°E , geomagnetic lat = -52°), as well as from Wallops Island (39°N , 76°W , geomagnetic latitude = 52°). The disturbance patterns in NmF_2 at Wallops Island match the negative phase patterns at Hobart, but considerable differences occur for the initial positive phase.

MDIT-06 Super Medium-Scale Traveling Ionospheric Disturbance observed at mid-latitude during the geomagnetic storm on November 10, 2004 - by Michi Nishioka

Status of First Author: Student IN poster competition PhD

Authors: M. Nishioka, A.Saito, T.Tsugawa

Abstract: Medium-Scale Traveling Ionospheric Disturbances (MSTIDs) whose peak-to-peak amplitude was larger than 20TECU were observed at mid-latitude during the geomagnetic storm on November 10, 2004. High resolution data of GPS Earth Observation Network (GEONET) clarify the characteristic of the Total Electron Content (TEC) fluctuations observed over Japan. The fluctuation started around 0930UT, followed by a TEC enhancement after the sunset. The fluctuations had several wave-fronts which extended from north-west to south-east and propagated from northeast to southwest. TEC data around Japan reveals that the fluctuation was mainly observed from 18° to 28° of the geomagnetic latitude in the both hemisphere. Those characteristics were same as those of Medium-Scale Travelling Ionospheric Disturbance (MSTID) in spite of the unusual large amplitude. TEC fluctuation was also observed by the Gravity Recovery and Climate Experiment (GRACE) satellites which flew at 470km altitude. The amplitude observed by the GRACE-A satellite was 5-12 TECU while that observed by ground-based GPS receivers was 8-12 TECU at 1340UT. Since those amplitudes were comparable, the altitude where the fluctuation of super MSTID occurred was estimated to be around and above 470km. Ion density observation by the Defense Meteorological Satellite Program (DMSP)-F15, and Challenging Minisatellite Recovery and Climate Experiment (CHAMP) satellites observed ion density fluctuations associating with the super MSTID at 850km and 360km altitudes, respectively. By comparing the ratio of the fluctuation to the background ion density, it is found that the super MSTIDs existed around 850km altitude and at higher altitude than 360km. Large amplitude of the super MSTIDs could be caused by uplift of the ionosphere. Strong eastward electric field can be a candidate of the uplift.

MDIT-07 Backscattered fraction of precipitating ionospheric photoelectrons - by Phil Richards

Status of First Author: Non-student

Authors: Phil Richards, George Mason University, Physics and Astronomy Department, 4400 University Drive, MSN 3F3 Fairfax, VA 22030, richards@cs.uah.edu, Bill Peterson, LASP, University of Colorado, Boulder, pete@lasp.colorado.edu

Abstract: The FAST electron spectrometer offers a serendipitous opportunity to determine for the first time the fraction of precipitating photoelectrons that are backscattered. Ionospheric photoelectrons produced by solar EUV radiation can escape into the plasmasphere and travel along magnetic field lines to the opposite hemisphere. In 2002 the FAST satellite orbit sliced through the plasmasphere above 3000 km altitude where it detected photoelectrons coming from both hemispheres with energies in the range ~10 to 800 eV. When one hemisphere is sunlit and the other is in darkness, the photoelectrons arriving at the satellite from the dark hemisphere are photoelectrons that are backscattered from the dark thermosphere after traveling from the sunlit hemisphere. This paper compares the measured and modeled backscattered fraction of photoelectrons. The backscatter ratio of precipitating photoelectrons is important for twilight airglow calculations.

MDIT-08 Clues to the properties of medium scale traveling ionospheric disturbances - by Ilgin Seker

Status of First Author: Student IN poster competition PhD

Authors: Ilgin Seker, John D. Mathews

Abstract: Perhaps the most persistent and prominent of the mid-latitude phenomena is the Medium-Scale Traveling Ionospheric Disturbances (MSTIDs) in the F-region. These MSTIDs have been given various other names such as: plasma depletion bands, plasma bubbles, slabs, and thermospheric waves. Using several instruments together to observe these MSTIDs proves to be very useful. In particular, the plasma structures seen in the narrow-beam ISR cannot be understood fully without the allsky images, which provide the horizontal context for the vertical radar results. Important results on the 3D geometry of these structures are found using a specific observation technique that is based on the combined incoherent scatter radar (ISR) and allsky imager observations of F-region MSTID structures over the Arecibo Observatory (AO) in Puerto Rico. In order to further confirm the findings on the 3D structure of these MSTID bands, a 3D model based on these observations is constructed. This empirical model is intended to replicate both the azimuth-scanning ISR and the allsky imager results, and will be especially useful in explaining how these complex structures appear in azimuth-scanning ISR results. The results will give a much broader perspective on nighttime, mid-latitude F-region and point to new ways of interpreting MSTID structures and how they appear in ISR results.

MDIT-09 The Aeronomy of N₂⁺ in the Earth's Ionosphere - by David Voglozin

Status of First Author: Student IN poster competition PhD

Authors: David Voglozin

Abstract: Although N₂⁺ is produced in large quantities in the Earth's Ionosphere, it is a minor species in the ionosphere because the loss rate is very large. It is the major source of NO⁺ below 200 km and a key player in both the ion and energy channels at all altitudes. The photochemistry of N₂⁺ has been controversial since the beginning of the Atmosphere Explorer analysis in the 1970s and 1980s. Historically, model N₂⁺ densities are typically a factor of 2 larger than measured densities. This paper reexamines the problem in the light of recent laboratory measurements of some key reaction rates.

MDIT-10 Initial Spatial Heterodyne Spectrometer observations of neutral oxygen emission at 844.6 nm over Millstone Hill - by Steven Watchorn

Status of First Author: Non-student PhD

Authors: S. Watchorn, J. Noto, L. S. Waldrop

Abstract: The Spatial Heterodyne Spectrometer (SHS) installed by Scientific Solutions, Inc., at Millstone Hill made its first observations of 844.6-nm neutral oxygen emissions in Spring 2008. These observations will be incorporated into a forward model to better characterize neutral winds in the thermospheric F-region. The SHS, which was recently field-widened to increase its

sensitivity, can clearly resolve the 844.636 and 844.676 nm lines of the 844.6 oxygen triplet, allowing it to distinguish two significant sources of 844.6-nm oxygen emission over Millstone Hill: photoelectron impact emission and Bowen fluorescence. The latest instrument modifications will be discussed, and spectra of initial observations will be presented.

MDIT-11 Midlatitude spread F - by Preeti Bhaneja

Status of First Author: Student IN poster competition PhD

Authors: Preeti Bhaneja, UT Dallas, Dr.G.D.Earle, UT Dallas, Dr.R.L.Bishop, The Aerospace Corp., Dr.P.A.Roddy, AFRL

Abstract: A statistical study of Midlatitude Spread F (MSF) at Wallops Island (37.8°N, 284.53°E) has been conducted. This study involves ground-based and in-situ data. Ionosonde data have been processed and the results show that MSF has a seasonal and a solar cycle variation. A rocket was launched into MSF from Wallops Island on October 30, 07 at 12:12 AM. Rocket data are currently being analyzed and will be used to determine electric field and wind direction measurements. This will give an insight into the small scale structure of the MSF instability.

Equatorial Ionosphere or Thermosphere

EQUI-01 Comparison of Coherent Backscatter and Airglow Images from Equatorial Plasma Depletions Shawn Adderly

Status of First Author: Student IN poster competition Undergraduate

Authors: Shawn A. Adderly, Ethan S. Miller, Jonathan J.Makela

Abstract: A study of the relationship between the spatial characteristics of Equatorial Plasma Bubbles (EPBs) observed in optical data and the intensity of radar backscatter has been conducted. We use imagery from the Cornell Narrow-Field Imager (CNFI) located atop the Haleakala Volcano on the island of Maui, HI, and radar data from a 50-MHz coherent scatter radar located at Christmas Island. These two locations are at the same magnetic longitude but different latitudes. Thus, this study represents an attempt to understand the relationship of irregularity structure at the magnetic equator to that a significant distance from the magnetic equator. We seek to demonstrate that the strongest backscatter from the radar occurs at locations that are magnetically connected to the center of EPBs observed in CNFI. Our study is based on imager and radar data collected from 2003 through 2007.

EQIT-02 Simultaneous Observations of Equatorial Ionospheric Plasma Bubbles from Two Sites during the SpreadFEx Campaign - by Narayan Prasad Chapagain

Status of First Author: Student IN poster competition PhD

Authors: Narayan P. Chapagain, Michael J. Taylor, Dominique Pautet (Center for Atmospheric and Space Sciences, Utah State University, Logan, UT)

H. Takahashi (Instituto Nacional de Pesquisas Espaciais (INPE), São José dos Campos, São Paulo, Brazil)

David C. Fritts (Colorado Research Associates, CO)

n.chapagain@aggiemail.usu.edu

Abstract: The equatorial SpreadF Experiment (SpreadFEx) campaign was carried out using a variety of instruments (all-sky imagers, digisondes, photometers, meteor/VHF radars, GPS receivers) at several sites in Brazil from September to November, 2005 supported by the NASA Living with a Star program. The main purpose of the campaign was to study the generation mechanism, development and spatial distribution of the ionospheric plasma bubbles. The Utah State University (USU) all-sky CCD imager operated at São João d'Aliação (14.8°S, 47.6°W), near Brasília, and the Brazilian imager at Cariri (7.4°S, 36°W) observed simultaneously the evolution of the ionospheric plasma bubbles in the OI (630 nm) emission. The two sites are ~1500 km apart approximately in the same magnetic latitude (Cariri at 8°S and Brasília at 9°S). Here we have summarized the results obtained during coincident observations from these two sites. The results show that the trends of the zonal velocities variations are similar at both sites but strong differences occurred in the development and distribution of the plasma bubbles between the two sites and during consecutive nights.

EQIT-03 Three-Dimensional Simulation of Equatorial Spread-F with Meridional Winds - by Jonathan Krall

Status of First Author: Non-student

Authors: J. Krall[1], J. D. Huba[1], G. Joyce[2], and S. T. Zalesak[1]

[1] Plasma Physics Division, Naval Research Laboratory, Code 6700, Washington, DC 20375-5346

[2] Icarus Research, Inc., P O Box 30780, Bethesda, MD 20824-0780

Abstract: The SAMI3 three-dimensional simulation code is used to examine the effect of meridional winds on the growth and suppression of equatorial spread-F. The simulation geometry conforms to a dipole field geometry that extends up to 1600 km at the equator and down to an altitude of 85 km, but extends over only 4 degrees in longitude. The full SAMI3 ionosphere equations are included, providing ion dynamics both along and across the field. The potential is solved in two dimensions in the equatorial plane under a field-line equipotential approximation. By selectively including terms in the potential equation, the reduced growth predicted by Maruyama[1] and the stabilization predicted by Zalesak and Huba[2] are separately realized. We find that a constant meridional wind of 60 m/s stabilizes spread-F.

[1] Maruyama, T., J. Geophys. Res., 93, 14,611–14,622, 1988

[2] Zalesak, S. T., and J. D. Huba, Eos Trans. AGU, 72, Spring Meet. Suppl., 211, 1991.

EQIT-04 Effect of meteor ionization on Sporadic-E observed at Jicamarca - by Akshay Malhotra

Status of First Author: Student IN poster competition PhD

Authors: Akshay Malhotra

Abstract: Relatively little progress has been made in the study of equatorial Sporadic-E when compared to the study of mid-latitude Sporadic-E. Indeed, it is unclear if Sporadic-E has been observed at all near the geomagnetic equator using any technique other than the ionosonde. We present here what we believe to be the first Sporadic-E (defined here as altitude-narrow E-region layers that last tens of minutes) observations from Jicamarca Research Observatory. The structure and characteristics of these equatorial Sporadic-E layers is compared with their mid-latitude counterparts. We also demonstrate the immediate effect of meteor-produced ionization on the formation and evolution of the equatorial Sporadic-E layers - a relationship that has been a source of much work and speculation in the community for over 70 years.

EQIT-05 Coherent scatter radar imaging observations of equatorial spread F in Brazil - by Fabiano S Rodrigues

Status of First Author: Non-student PhD

Authors: Fabiano S Rodrigues 1,2; David L Hysell 1; Eurico R de Paula 3

1. Cornell University, Ithaca, NY

2. Now at ASTRA, San Antonio, TX

3. INPE, Sao Jose dos Campos, Brazil

Abstract: We will be presenting coherent scatter radar images of equatorial spread F structures observed with a small, low-power radar in Sao Luis, Brazil. Initial analysis of the observations made during the spreadF Experiment (spreadFEx) campaign (Fritts et al. 2008) produced radar images of the so-called bottom-type layers and radar plumes. Clusters of bottom-type layers were observed preceding the occurrence of radar plumes. These clusters can be associated with density perturbations caused by a shear-driven instability operating in the bottom-side F-region as suggested by Hysell and Kudeki (2004). Furthermore, these clusters seem to provide useful diagnostics for spread F forecast.

EQIT-06 Massively Parallel Simulations of Gradient Drift Waves in the E-region Ionosphere - by Yann Tambouret

Status of First Author: Student IN poster competition PhD

Authors: Yann Tambouret, Meers Oppenheim, Center for Space Physics, Boston University

Abstract: Radar observations of Type 1 and 2 echoes from E region plasma irregularities have been explained by the Farley-Buneman (FB) and Gradient-Drift (GD) instabilities. Short wavelength instabilities are predominantly attributed to FB instabilities, whereas long wavelength instabilities result from GD instabilities. Since radars only detect relatively short wavelength

irregularities (~ 15 m), indirect measurements of long GD waves rely upon either a nonlinear cascade from longer to shorter waves or a GD field strong enough to drive a directly observable FB turbulence. Short wavelength waves include important ion kinetic effects, but purely kinetic simulations are expensive, particularly when resolving the long-times and large-scales appropriate for the GD instability. To investigate these coupling mechanisms, we have developed a massively parallel hybrid kinetic/fluid simulator capable of dividing the simulation effort across thousands of processors with a high level of efficiency. To reduce the computational cost, we model the electron component of the plasma using a standard 5-moment approximation while the kinetic details of the ions are reproduced using a particle-in-cell algorithm.

EQIT-07 Estimating electric fields in the equatorial ionosphere from CHAMP observations - by Patrick Alken

Status of First Author: Student IN poster competition PhD

Authors: Patrick Alken (NOAA, NGDC, patrick.alken@noaa.gov), Stefan Maus (NOAA, NGDC, stefan.maus@noaa.gov)

Abstract: The day-time eastward equatorial electric field (EEF) in the E-region plays an important role in equatorial ionospheric dynamics. It is responsible for driving the equatorial electrojet (EEJ) current system, equatorial vertical ion drifts, and the equatorial ionization anomaly (EIA) among others. Due to its importance, there is much interest in accurately measuring the EEF. However, there is a severe lack of high quality data with the notable exception being the JULIA coherent scatter radar in Peru. In this work we use CHAMP satellite-derived latitudinal current profiles of the day-time EEJ in order to estimate the eastward electric field at all longitudes, seasons, and day-side local times. We have constructed a dataset of over 32,000 EEF estimates based on six years of CHAMP data. Our estimates agree well with JULIA measurements, with an RMS error of 0.13 mV/m.

EQIT-08 Wind dynamo effects on ground magnetic perturbation and vertical drifts - by Tzu-Wei Fang

Status of First Author: Student IN poster competition PhD

Authors: Tzu-Wei Fang

Abstract: The equatorial electrojet (EEJ) flows as an enhanced eastward current in the daytime E region ionosphere between 100 and 120 km height at the Earth's magnetic equator. The flowing currents in the ionosphere induce magnetic perturbations on the ground. Calculating the difference between the horizontal components of magnetic perturbation (H) at magnetometers near the equator and about 6-9 degrees away from the equator, ΔH , provides us an indicator of the strength of the EEJ. However, in this research we use model simulation to address that the wind dynamo can also be an important factor in changing the magnitude of ΔH . The NCAR Thermosphere-Ionosphere-Electrodynamics General Circulation Model (TIE-GCM) is applied to perform the simulation. Through modifying the neutral wind and high latitude magnetic potential in March equinox under moderate solar activity ($F_{10.7} = 140$ units), the latitudinal distributions of H , diurnal variations of ΔH and vertical drift in the Peruvian ($76^\circ W$) are presented in this paper. The relationship between ΔH and vertical drift are also discussed which helps us to understand the importance of the EEJ and wind dynamos in altering the relation. Model results show the altitude variation of wind velocity in the low latitude region is capable of modifying the ground magnetic perturbation at the location few degrees away from the equator. Only combine both the wind dynamo effect and the strength of EEJ, the magnitude of ΔH and its relation with vertical drift can be better estimated.

EQIT-09 Improved E-region electron density and meridional wind measurements over Jicamarca using multi-static configurations - by Freddy Galindo, presented by Karim Kuyeng

Status of First Author: Non-student

Authors: Freddy Galindo

Abstract: At equatorial latitudes standard incoherent scatter radar techniques used at other latitudes, cannot be used routinely to diagnose the E region. This limitation is mainly due to the presence of strong coherent echoes from equatorial electrojet (EEJ) field-aligned irregularities. In recent years, a variety of radar techniques have been developed at the Jicamarca Radio Observatory (JRO) to make use of the strong EEJ echoes to diagnose the E region. Given the strong EEJ echoes, particularly during the day, all of these techniques make use of small antenna systems with grating-lobe array and/or bistatic configurations, allowing daytime

measurements of electric fields, and zonal neutral wind and electron density profiles. Measurements at night (including sunrise and sunset times) have not been possible due to the poor sensitivity of the systems used.

In this work, we propose to use specular meteor echoes using JRO's large power-aperture for transmission and small interferometric systems for reception few tens to hundreds of kms south and east of Jicamarca. The detection and identification of the specular echoes will be done in a similar manner to the traditional all-sky meteor systems, allowing the direct measurement of the horizontal winds. Moreover, by using cross-polarized antennas on reception, the phase difference, due to Faraday rotation, between orthogonal polarizations will provide the total-electron content until the scattering point. Compared to standard all-sky meteor systems, the multistatic measurements will be done on a very small volume avoiding the assumption of a homogeneous wind field on a large area. The use of meteor echoes will allow measurements at night. Moreover, since the Bragg wavelength of the multistatic system is larger than the monostatic system, better sensitivity is expected as well as higher altitude coverage. Finally, as a by product of this experiment, we'll be able to study the three known meteor echoes at the same time, i.e., meteor-head, non-specular meteor trail, and specular meteor trail. Preliminary results using a receiver station ~250 km south of Jicamarca will be presented and discussed.

EQIT-10 630.0 nm airglow observations at mid-latitudes – by Carlos Martinez

Status of First Author: Non-student

Authors: C.Martinis, J.Baumgardner, J.Wroten, M.Mendillo

Boston University operates an all-sky imager (ASI) located at Arecibo, Puerto Rico. Typical observations show dark/bright bands tilted with respect to the geomagnetic meridian moving south-westward. These mid-latitude features are associated with the Perkins or coupled Es-F region instabilities, commonly known as medium scale traveling ionospheric disturbances (MSTIDs). Other processes observed, less frequently, are related to airglow depletions associated with the Rayleigh-Taylor instability (RTI). We present here a summary of the different optical processes observed at this station, and compare with similar phenomena observed at different longitudinal sectors.

EQIT-11 Low Latitude Storm Time Electric Fields and their Role in the Coupled Thermosphere-Ionosphere Plasmasphere System - by Naomi Maruyama

Status of First Author: Non-student

Authors: N. Maruyama¹, T. Fuller-Rowell¹, M. Codrescu¹, D. Anderson¹, A. Richmond², A. Maute², S. Sazykin³, F. Toffoletto³, R. Spiro³, R. Wolf³, and G. Millward⁴

1: University of Colorado, CIRES, and NOAA, SWPC, Colorado, USA (Naomi.Maruyama@noaa.gov)

2: National Center for Atmospheric Research, High Altitude Observatory, Colorado, USA

3: Rice University, Physics and Astronomy Department, Texas, USA

4: University of Colorado, LASP, Colorado, USA

Abstract: We have developed a self-consistent first-principles model of the inner magnetosphere and thermosphere-ionosphere-plasmasphere, in order to understand the response of the electrodynamic interactions within the coupled system and the role of the electrodynamic in restructuring the ionosphere, plasmasphere and thermosphere, in particular, during geomagnetically active conditions. Modeling of the storm-time ionospheric electrodynamic requires a description of the two disturbance mechanisms: prompt penetration and disturbance dynamo. We have coupled the Rice Convection Model (RCM), used to calculate the region 2 field aligned currents from the inner magnetosphere which control the shielding process of the high latitude convection electric field, and the Coupled Thermosphere Ionosphere Plasmasphere electrodynamic (CTIPE) model, used to calculate the time-dependent conductivities and neutral winds that are the key to describe the disturbance dynamo as well as the quiet-time ionospheric wind dynamo. Self-consistency in the electrodynamic coupling between RCM and CTIPE is accomplished by using a common global electrodynamic solver. As compared to the classical picture of prompt penetration, our model results from the non self-consistent coupling suggest a possibility that penetration effects can have a longer lifetime when the IMF B_z is large and southward, as a consequence of the ineffective shielding resulted from the magnetospheric reconfiguration. Furthermore, our simulations indicate that the arrival of the disturbance dynamo effect in the low latitude ionosphere can possibly be faster than previously believed, as the disturbance dynamo is modified by the changes in the conductivity and neutral wind initiated by the penetration effect. Comparison of the results from the combined models with observations under a variety of conditions demonstrates that our models are capable of reproducing many of the observed features in the ionosphere. In this paper, the

electrodynamic interactions will be discussed using the fully self-consistently coupled model, and its impact on the low latitude coupled ionosphere- thermosphere system.

EQIT-12 Variability of Zonal Ion Drifts During Storm-Times at Equatorial Latitudes - by Edgardo Pacheco

Status of First Author: Student IN poster competition PhD

Authors: Edgardo Pacheco, R.A. Heelis

Abstract: We utilize measurements from the DMSP and ROCSAT-1 satellites from the years 2000-2004 to investigate the storm time dynamics of the equatorial topside ionosphere at different local times and longitudes during the same events. Our study focuses on the local time variation of the zonal ion drift perturbations. The DMSP F13 and F15 satellite data are gathered consistently at four different local times (1800, 0600, 2100 and 0900) at the equator near 800 km altitude. ROCSAT-1 provided data at additional local times near 600 km altitude and also at the same local times as DMSP. We have selected data from storms for which the values of the Dst index are less than -200 nT in order to determine the appearance of systematic repeatable storm time behavior observed in satellite measurements.

EQIT-13 Longitudinal Structure of the Low-Latitude F-Region Ionosphere - by Nicholas Pedatella

Status of First Author: Student IN poster competition PhD

Authors: N. M. Pedatella, J. M. Forbes, J. Lei, J. Thayer, and K. M. Larson

Abstract: Changes in the longitudinal structure of the equatorial ionization anomaly (EIA) are investigated using in-situ electron densities from the CHAMP satellite. Intra-annual variability and changes due to enhanced geomagnetic activity are both considered. The dominant longitudinal structures of the EIA are found to be wave-2, wave-4 and wave-3 in January, July, and December, respectively. The leading nonmigrating tidal components in the equatorial zonal wind at 100 km derived from the SABER/TIDI instruments on the TIMED satellite during these same time periods are the westward propagating semidiurnal tide with zonal wavenumber 4 (SW4), and the eastward propagating diurnal tides with zonal wavenumbers 3 (DE3) and 2 (DE2). When viewed at a fixed local time SW4, DE3, and DE2 appear as wave-2, -4, and -3, respectively. The intra-annual changes observed in the longitudinal structure of the F-region ionosphere are therefore attributed to changes in the various nonmigrating tides at E-region altitudes. We further explore the disruption of the dominant wave-4 structure of the EIA due to a sequence of three coronal mass ejections that occurred during July 2004. Significant longitudinal structure is not evident during the initial-main phases of the storms and the wave-4 structure reappears as the primary component during the recovery phase. Storm-time changes in the electric fields, neutral winds, and neutral composition are thought to be responsible for the observed disruption of the longitudinal structure of the EIA. The results indicate that the sampling longitude needs to be accounted for when using satellite observations at a fixed local time for geomagnetic storm studies.

EQIT-14 Altitude Variation of the OII 7320Å spectral line width at Arecibo - by Pedrina Terra

Status of First Author: Non-student

Authors: Pedrina Terra , J. Noto, M. Migliozzi, J. Riccobono, C. G. M. Brum, R. Garcia, E. Robles and R. Kerr

Abstract: The excited O⁺ (2P) atom is formed by photoionization or electron impact with energy in excess of 18.6 eV (< 666Å). With a lifetime of 4.57s in the upper state and no local source in the earth's shadow, the O⁺(2P) to O⁺(2D) transition produces a twilight airglow at 7320Å and 7330Å very near to the solid-earth shadow line. The emission has therefore been used in the past to determine the altitude profile of O⁺ temperature at the terminator, using high spectral resolution detection. Some of these measurements have been interpreted to imply a population of hot oxygen atoms in the upper thermosphere and lower exosphere. That population remains speculative, but has the potential, if it exists, to confuse ISR ion temperature fits, with hot O⁺ spectra having similar width to He⁺ spectra. Using CCD array detection with a high-spectral resolution Fabry-Perot interferometer, we achieve a 40-fold enhancement in sensitivity at 7320Å over earlier work, by virtue of an 85-90% quantum efficiency and 4-order simultaneous sampling. Problematic OH contamination is eliminated by use of a very narrow 3.0Å FWHM interference filter, and 0.9cm Fabry-Perot plate spacing achieves a spectral resolution of 0.032Å, the emission doublet line width at 7320Å for any temperature greater than 200K. OII 7320Å line width data acquired at Arecibo (18o.35 N, 66o.75W) since March of 2008 during evening and morning twilights using this configuration and analysis are presented in this work.

Index

Acebal, Ariel, 8
Adderly, Shawn, 22
Alken, Patrick, 24
Anderson, Callum, 13
Armstrong, Shaun, 5
Azeem, Irfan, 15

Bekerat, Hamed, 15
Bhaneja, Preeti, 22
Briczinski, Stanley, 18
Brum, Christiano, 6
Burns, Alan, 19
Butler, Thomas, 13

Chapagain, Narayan, 22
Clemmons, James, 1
Conde, Mark, 13
Cooper, Shaun, 13

Datta-Barua, Seebany, 8
Diaz, Marcos, 12
Didebulidze, Goderdzi, 6
Drake, Kelly, 9
Dymond, Ken, 4

Emery, Barbara, 8

Fallen, Christopher, 15
Fang, Tzu-Wei, 24
Fernandez, Jose, 14

Galindo, Freddy, 24
Gaulden, Travis, 16
Grebowsky, Joseph, 19

Holmes, Jeffrey, 14
Huang, Cheng-Yung, 1

Krall, Jonathan

Lai, Peichen, 16
Lei, Jiuhou, 9
Luan, Xiaoli, 19
Lundberg, Erik, 16

Malhotra, Akshay, 23
Mannucci, Anthony, 10
Martinis, Carlos, 25
Maruyama, Naomi, 25

Maute, Astrid, 17
Mende, Steve, 3

Meriwether, John, 1
Michell, Robert, 12
Mierkiewicz, Edwin, 2
Minin, Serge, 2

Narvaez, Clara, 20
Nishioka, Michi, 20
Nossal, Susan, 7
Noto, John, 7

O'Hanlon, Brady, 10

Pacheco, Edgardo, 26
Parris, Richard, 5
Pawlowski, David, 10
Pedatella, Nicholas, 26
Pilinski, Marcin, 2

Qian, Liying, 11

Redmon, Rob, 3
Richards, Phil, 21
Roach, Kate, 11
Robles, Eva, 6
Rodrigues, Fabiano, 23

Seker, Ilgin, 21
Spaletta, Jeffrey, 5
Sutton, Eric, 11

Tambouret, Yann, 23
Terra, Pedrina, 26

Voglozin, David, 21

Wang, Wenbin, 11
Watchorn, Steven, 21
Watts, Christopher, 4
Wu, Qian, 17

Yonker, Justin, 12

Zabotin, Nick, 4, 5
Zettergren, Matt, 17
Zou, Shasha, 18

